ACS NANO

www.acsnano.org

REVIEW

Chirality-Controlled Synthesis and Applications of Single-Wall Carbon Nanotubes

Bilu Liu,[†,‡,#] Fanqi Wu,[§,#] Hui Gui,[§] Ming Zheng,[*,∥] and Chongwu Zhou[*,†,§]

[†]Department of Electrical Engineering and [§]Department of Chemical Engineering and Materials Science, University of Southern California, Los Angeles, California 90089, United States

[‡]Tsinghua-Berkeley Shenzhen Institute (TBSI), Tsinghua University, Shenzhen, Guangdong 518055, P. R. China

[∥]National Institute of Standards and Technology, Gaithersburg, Maryland 20899, United States

ABSTRACT: **Preparation of chirality-defined single-wall carbon nanotubes (SWCNTs) is the top challenge in the nanotube field. In recent years, great progress has been made toward preparing single-chirality SWCNTs through both direct controlled synthesis and postsynthesis separation approaches. Accordingly, the uses of single-chirality-dominated SWCNTs for various applications have emerged as a new front in nanotube research. In this Review, we review recent progress made in the chirality-controlled synthesis of SWCNTs, including metal-catalyst-free SWCNT cloning by vapor-phase epitaxy elongation of purified single-chirality nanotube seeds, chirality-specific growth of SWCNTs on bimetallic solid alloy catalysts, chirality-controlled synthesis of SWCNTs using bottom-up synthetic strategy from carbonaceous molecular end-cap precursors, *etc.* Recent major progresses in postsynthesis separation of single-chirality SWCNT species, as well as methods for chirality characterization of SWCNTs, are also highlighted. Moreover, we discuss some examples where single-chirality SWCNTs have shown clear advantages over SWCNTs with broad chirality distributions. We hope this review could inspire more research on the chirality-controlled preparation of SWCNTs and equally important inspire the use of single-chirality SWCNT samples for more fundamental studies and practical applications.**

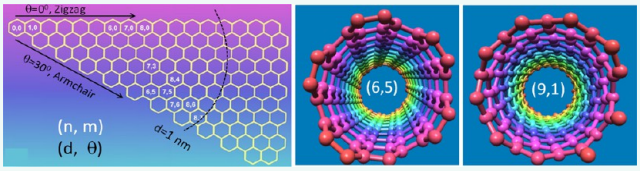

KEYWORDS: *single-wall carbon nanotube, graphene, chirality, handedness, diameter, electronic property, controlled growth, separation*

Carbon nanotubes (CNTs),[1] especially single-wall carbon nanotubes (SWCNTs),[2−4] have been extensively studied due to their excellent mechanical, chemical, electronic, optical, and thermal properties and their potential use in various fields including composites, electronics and optoelectronics, biological and medical applications, energy harvest and storage, among many others.[5] At this stage, industrial-scale production[6−8] of CNTs has been realized after extensive research,[9−11] and several CNT-based products have been commercialized, mainly using multiwall CNTs (MWCNTs).[12] On the other hand, applications of SWCNTs are still rare, where one of the key hurdles is the structure and property heterogeneity problem in current SWCNT products.

A SWCNT can be viewed as a rolled-up tube from a graphene sheet (Figure 1a). Depending on the way the graphene sheet is rolled up, the resulting SWCNT can have very different structures, *i.e.*, atom arrangements in the three dimensions. The structure of a SWCNT can be described by its chirality (n,m) or, equivalently, diameter (d) and chiral angle (θ). Figure 1b,c shows the atomic structure of (6,5) and (9,1) SWCNT, respectively. It is well-known that electronic band structures and many properties of SWCNTs are determined by their chiralities. For example, about one-third of SWCNTs are metals (when $n - m = 3q$, here q is an integer), while the rest of the two-thirds are semiconductors (when $n - m \neq 3q$). Equally noticeable is that for semiconducting SWCNTs, their band gaps are inversely proportional to tube diameters. Therefore, the structure and property of SWCNTs, including diameter, chirality, and electronic properties, have to be well controlled for various applications of nanotubes. Among these tasks, chirality control is the most difficult one. In the past two decades, tremendous efforts have been devoted to this direction with great success. Nowadays, researchers are able to prepare SWCNT samples with highly enriched single-chirality species, through either direct controlled growth or postsynthesis separation approaches or a combination of both. On the other hand, there is increasing interest in studying chirality-dependent properties and applications of SWCNTs, especially in electronics and optoelectronics, energy, and biorelated fields. Such chirality-dependent studies benefit greatly from the success in obtaining single-chirality SWCNT samples. These successes also call for more efforts in single-chirality SWCNT preparation, especially by direct synthesis approaches that could potentially provide both high quality and large quantity. In this Review, we provide an up-to-date overview of the major

Received: October 13, 2016
Accepted: December 30, 2016

DOI: 10.1021/acsnano.6b06900
ACS Nano XXXX, XXX, XXX−XXX

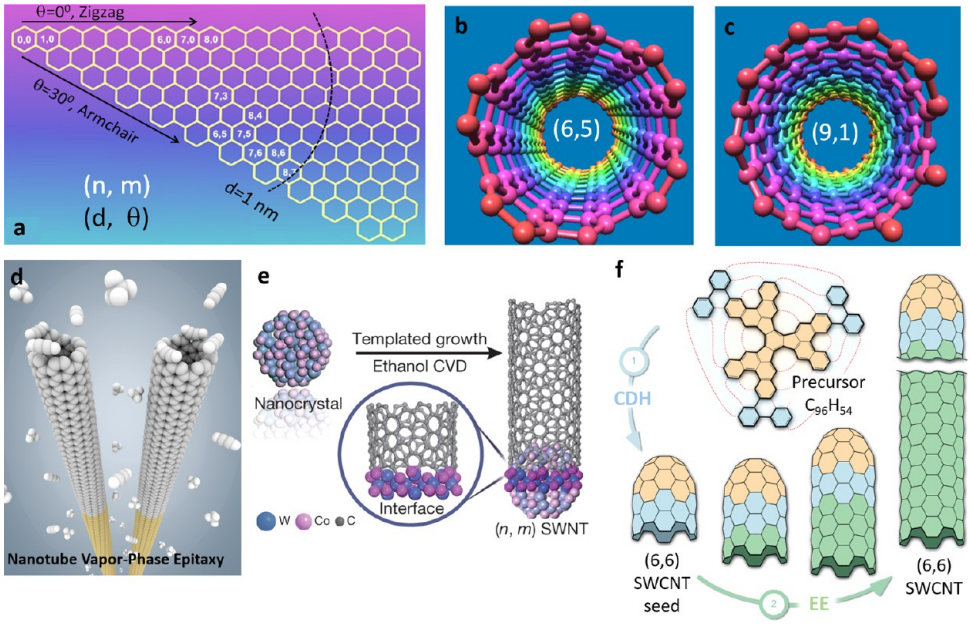

Figure 1. Structure of SWCNTs and recent major achievements on the chirality-controlled synthesis of SWCNTs. (a) Chirality map of SWCNTs where key parameters such as the chiral index, chiral angle, and diameter, are shown. (b, c) Atomic structure of (6,5) and (9,1) SWCNT, respectively. (d) Schematic illustration of metal-catalyst-free SWCNT cloning by vapor-phase epitaxy elongation of single-chirality nanotube seeds.[13,16] (e) Schematic illustration of the chirality-specific growth of SWCNTs on W−Co bimetallic solid alloy catalysts.[14] Reproduced with permission from ref 14. Copyright 2014 Nature Publication Group. (f) Schematic illustration of the chirality-controlled growth of SWCNTs using bottom-up synthetic strategy from molecular end-cap precursors.[15] Reproduced with permission from ref 15. Copyright 2014 Nature Publication Group.

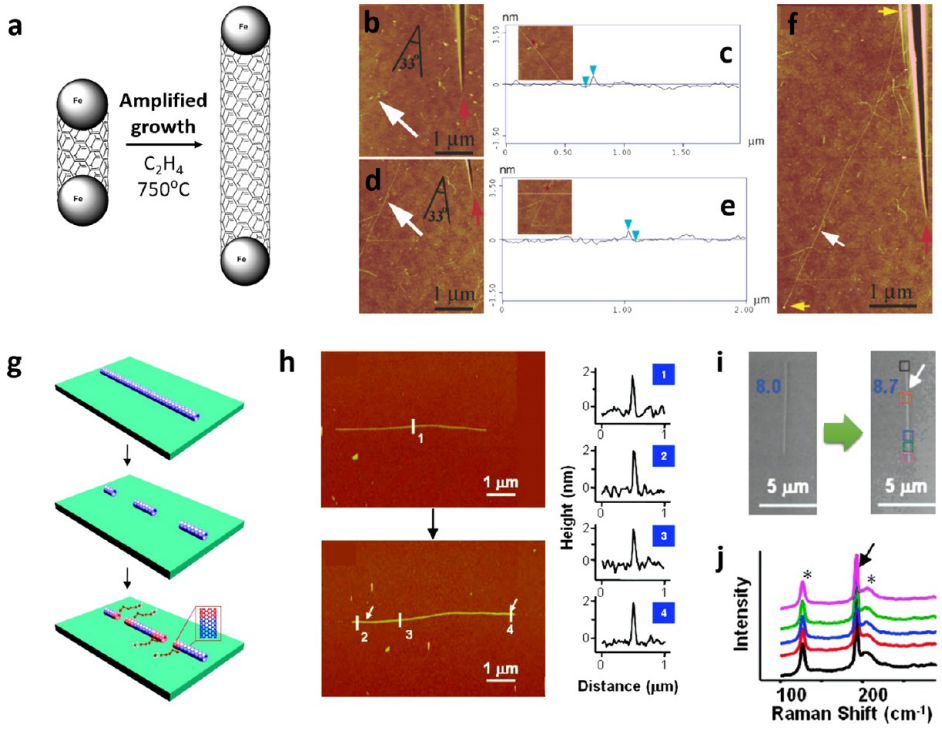

Figure 2. Chirality-controlled synthesis of SWCNTs using short nanotube segments as the growth template *via* VLS amplification and cloning process. (a) Schematic diagram of the VLS amplification growth process using an Fe-docked SWCNT as the growth template.[32] (b−f) AFM images and analysis of SWCNTs before (b and c) and after amplification growth process (d−f). (a−f) Reproduced with permission from ref 32. Copyright 2006 American Chemical Society. (g) Schematic diagram showing the SWCNT cloning process using e-beam lithography cut nanotube segments as the template.[34] (h) AFM images and height profiles of SWCNTs before and after the cloning process. (i) SEM image of a SWCNT before and after cloning. (j) RBM region Raman spectra across the SWCNT in panel i which shows the unchanged RBM shift at 192.8 cm^{-1}. Peaks marked by * come from the quartz substrate. (g−j) Reproduced with permission from ref 34. Copyright 2009 American Chemical Society.

DOI: 10.1021/acsnano.6b06900
ACS Nano XXXX, XXX, XXX−XXX

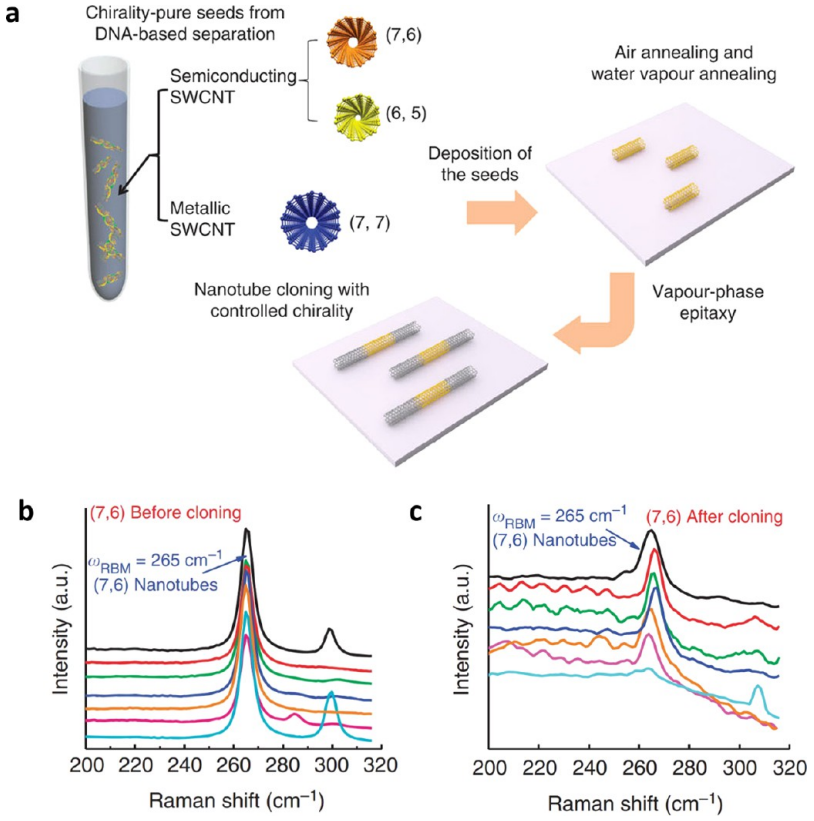

Figure 3. Chirality-controlled synthesis of SWCNTs using the VPE approach.[13] (a) Schematic diagram of the VPE process for the chirality-controlled synthesis of SWCNTs. (b, c) RBM-region Raman spectra of (7,6) nanotubes before and after VPE process. (a–c) Reproduced with permission from ref 13. Copyright 2012 Nature Publication Group.

achievements on the chirality-controlled preparation of SWCNTs, with an emphasis on the direct growth approaches. Specifically, we review chirality-controlled synthesis of SWCNTs by various approaches, including metal-catalyst-free SWCNT cloning using vapor-phase epitaxy (VPE) elongation of purified single-chirality nanotube seeds[13] (Figure 1d), chirality-specific growth of SWCNTs on bimetallic solid alloy catalysts[14] (Figure 1e), chirality-controlled synthesis of SWCNTs using bottom-up synthetic strategy from carbonaceous molecular end-cap precursors[15] (Figure 1f), and so on. Meanwhile, the use of single-chirality or chirality-enriched SWCNTs for various applications, which appears to be an emerging direction that deserves more attention, has also been discussed. At the end of the Review, we point out some challenges in the field and opportunities lying ahead.

CHIRALITY-CONTROLLED SYNTHESIS OF CARBON NANOTUBES

Direct synthesis of SWCNTs with defined chirality has long been a sought-after goal for two decades. The chirality of a SWCNT is believed to be fixed at the nucleation stage as evidenced by the unchanged chirality along long SWCNTs.[17] Therefore, controlling the nucleation step during nanotube growth is crucial to realize chirality control. In principle, many parameters involved in CNT synthesis can have influence on the nucleation and consequently chirality distribution of as-grown CNTs, including types of catalysts,[7,13−15,18,19] carbon sources,[20,21] growth temperatures,[20,22−26] the carrier gas composition,[20,27,28] system pressure,[7] growth time,[29] *etc.* In reality, judging from the results researchers have reported so far, it is clear that catalysts have the most deterministic role on the chirality of as-synthesized CNTs. The reported methods for controlling nucleation and chirality can be grouped into three major classes: (i) seeded growth using CNT segments as growth templates; (ii) catalytic growth using elaborately chosen nanoparticle-based catalysts with desired chemical composition, size, structure, and high-temperature stability; and (iii) growth initiated from carbonaceous molecular seeds.

Seeded Growth Using Carbon Nanotube Segments as the Growth Templates. Seeded growth from short CNT segments is a promising approach to realize the exclusive production of any specific single-chirality SWCNTs starting from a small amount of nanotube seeds, considering recent success in single-chirality-based nanotube separation.[30,31] In this way, synthesis and separation can be combined together into a single method aiming for single-chirality SWCNTs. As early as in 2005, Smalley *et al.* reported the use of Fe nanoparticle (NP)-docked short SWCNTs as growth templates and realized the growth of much longer nanotubes *via* vapor–liquid–solid (VLS) amplification process (Figure 2a).[32] Atomic force microscopy (AFM) analysis indicated that the elongated parts of SWCNTs possessed the same diameter and surface orientation with the nanotube seeds (Figure 2b–f), although it was not known whether the chirality changed or not during the amplification process. Nevertheless, there is no doubt that this work opened up a possibility to realize chirality-controlled synthesis of SWCNTs *via* seeded growth from CNT templates or potentially other carbonaceous molecular seeds. In another work, they used a similar approach and started with open-end SWCNT arrays followed by reductively docking the nanotubes with Fe NPs.[33] Then they used the Fe-docked SWCNT arrays

DOI: 10.1021/acsnano.6b06900
ACS Nano XXXX, XXX, XXX–XXX

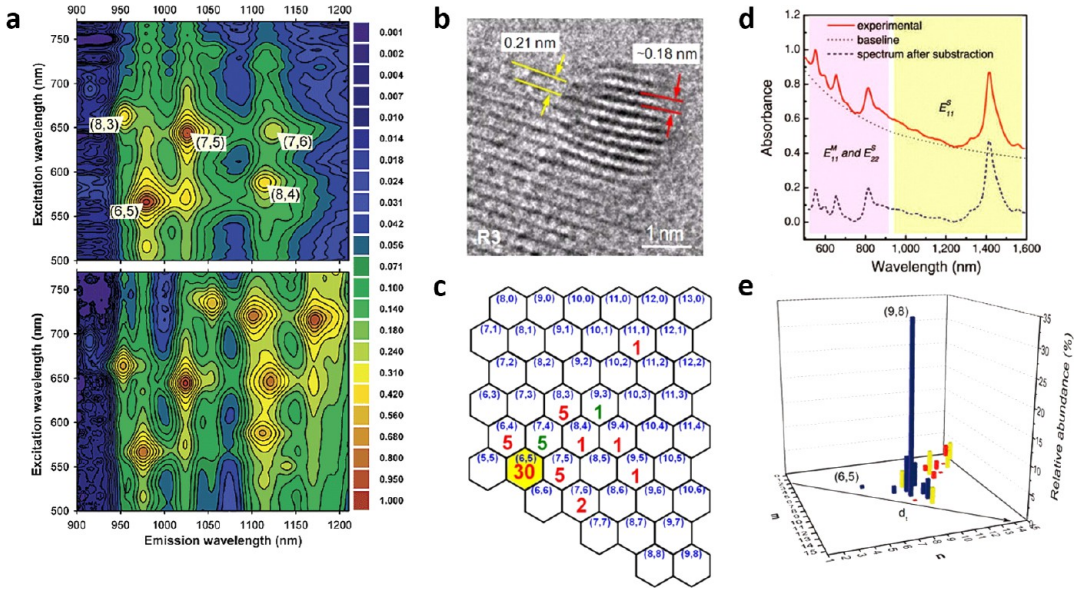

Figure 4. Chirality-controlled synthesis of SWCNTs *via* various catalyst engineering approaches. (a) Contour plots of normalized fluorescence intensities for CoMoCat sample[7] (top) in comparison with HiPco sample (bottom). Reproduced with permission from ref 7. Copyright 2003 American Chemical Society. (b) High-resolution transmission electron microscope image showing the lattice-mismatched epitaxial relationship between a Co nanoparticle and the MgO matrix.[42] (c) A chirality map of the SWCNTs grown on $Co_xMg_{1-x}O$ catalysts with the occurrence of a (*n*,*m*) nanotube labeled in its corresponding hexagonal cell, measured from electron diffraction analysis of 57 individual SWCNTs. (b, c) Reproduced with permission from ref 42. Copyright 2013 Nature Publishing Group. (d) Optical absorbance spectra of SWCNTs grown with $CoSO_4/SiO_2$ catalyst after catalyst reduction at 540 °C.[19] (e) Relative abundance of SWCNTs produced from the same catalyst, quantified by three characterization techniques including PL (blue), Raman (red), and absorption (yellow). (d, e) Reproduced with permission from ref 19. Copyright 2013 American Chemical Society.

for VLS amplification growth. Raman analysis indicated the epitaxially grown SWCNTs inherited the diameter and chirality on bulk amount of samples.

Later, an exciting approach using metal-free open-end SWCNTs as the growth template to aim for chirality-controlled synthesis *via* an open-end growth mechanism, named "cloning", was reported by Zhang, Liu *et al.*[34] They used short CNT segments with random chiralities, which were cut from long CNTs, to initiate the growth of the "new/duplicated" nanotubes without metal catalysts (Figure 2g). AFM and scanning electron microscopy (SEM) images showed that around 9% of seeds were elongated successfully. The yield was improved to 40% by using quartz as the growth substrate instead of SiO_2/Si. From the AFM analysis, the "new/duplicated" CNTs had the same diameters with the seeds (Figure 2h). Micro-Raman analysis further indicated that the newly grown CNT segments had the same radial breathing modes (RBMs) with the mother CNTs, indicating that the chirality of CNTs was preserved during the process (Figure 2i,j). This work suggests a potential strategy to grow CNTs with controlled chirality *via* a metal-free open-end mechanism.

Recently, our group has achieved direct synthesis of single-chirality SWCNTs with predefined chirality by combining SWCNT separation with chemical vapor deposition (CVD) synthesis together.[13] In our method, which we called VPE, we started with DNA-separated single-chirality SWCNT seeds.[30,31] Three different single-chirality (7,6), (6,5), and (7,7) CNT seeds, with purity higher than 90%, were used as growth templates for the following metal-free VPE growth using CH_4 or C_2H_5OH as the carbon sources (Figure 3a). Based on the AFM and SEM analysis, the nanotube seeds have been significantly elongated by a factor of ~100, from a few hundred nanometers to tens of microns. We note that Raman spectroscopy can determine the chirality of SWCNTs unambiguously only for small-diameter CNTs. In contrast, for large-diameter CNTs (>1.2 nm), there exist lots of uncertainties in using Raman alone to determine the chirality of a SWCNT, because multiple (*n*,*m*) chiralities can have very similar RBM positions and may be in resonance with the incident laser. Our Raman analysis unambiguously showed the chirality of the as-grown SWCNTs inherited the chirality of the nanotube seeds (Figure 3b,c), demonstrating controlled growth of CNTs with predefined chirality. The semiconducting nature of the as-grown (7,6) and (6,5) CNTs was confirmed using field-effect transistor (FET) measurements. Later, we found that by adding a small amount of C_2H_4 into CH_4 as the carbon source, we could increase the yield of VPE process significantly and have successfully grown SWCNTs of seven different chiralities, including armchair (6,6), (7,7), near-armchair (6,5), (7,6), medium-chiral-angle (8,3), and near-zigzag (9,1), (10,2) species.[16] We also observed chirality-dependent growth and termination behaviors of SWCNTs in the VPE process, which will be discussed later. Afterward, Homma *et al.* reported a similar strategy using DNA-separated CNT seeds as the growth templates for VPE regrowth of SWCNTs by both hot-wall and cold-wall CVD methods.[35] Systematic studies have been conducted to optimize the pretreatment conditions, carbon sources, and growth substrates. As a result, dense, long, and well-aligned CNTs were synthesized from seeds on quartz substrates by using a mixture of ethanol and acetylene at 850 °C, under optimum pretreatment conditions to activate the ends of seeds.[35] Raman analysis was employed to characterize the chirality of the as-grown SWCNTs, indicating the grown SWCNTs preserved the chirality from the short nanotube seeds. In addition to the traditional hot-wall CVD system, the cold-wall CVD system was also able to achieve the regrowth of

DOI: 10.1021/acsnano.6b06900
ACS Nano XXXX, XXX, XXX−XXX

nanotubes from seeds, suggesting this strategy is robust and independent of specific CVD systems. The VPE-cloning-based approach could in principle solve the nanotube chirality problem. However, the yield of VPE-grown CNTs is still low at this moment, which limits many mechanistic studies of the process and the use of such chirality-pure SWCNTs for applications. We envision that by using three-dimensional (3D) porous substrates or floating CNT seeds in gas phase, we may be able to increase the yield of the VPE cloning. Such studies are ongoing in our laboratories.

Metal-Nanoparticle-Based Catalysts for Single-Chirality Nanotube Synthesis. During the early days of nanotube research (before ~2005), the community generally believed that only iron-group metals, Fe, Co, and Ni, can catalyze SWCNT growth. Later on, numerous other metal NPs, including Cu, Ag, Au, Pd, Pt, Mn, *etc.*,[36−41] were also found to be able to grow SWCNTs. However, it is impossible to produce tiny metal NPs with identical sizes, structures, and compositions. Furthermore, during CNT growth stage at high temperatures, metal catalyst NPs are usually not stable and would change their properties through several mechanisms. The above features would bring uncertainties to CNT growth and make chirality-controlled growth of CNTs challenging when using metal NP catalysts. In order to realize good chirality control, the precise control of catalyst composition, size, structure, and especially its high-temperature stability is essential.

Increasing interactions between catalyst support and catalyst NPs by "anchoring" catalyst NPs on the support is an effective way to mitigate the property changes of metal NPs. Chirality-selective synthesis of SWCNTs using a silica-supported Co−Mo catalyst (CoMoCAT) was realized by Resasco *et al.*[7] Selective growth of (6,5) and (7,5) nanotubes was achieved, together comprising 57% of all semiconducting SWCNTs in the as-grown samples estimated from photoluminescence (PL) intensities (Figure 4a). The interaction between Co and Mo oxides was believed to play an important role in preventing Co NPs from aggregation at high temperatures. Later on, the same group further optimized the gaseous feed composition, growth temperature, and catalyst support and increased the selectivity of (6,5) nanotubes to 55%.[20] The successful realization of chirality-selective synthesis of (6,5) nanotubes with a relatively good selectivity using CoMoCAT has drawn great attention to solid-supported catalyst systems.

Besides using porous substrates, active catalyst NPs can also be stabilized by using various other methods. Fouquet *et al.* developed a much simpler approach for the selective growth of (6,5) SWCNTs.[22] They started with a thermally evaporated ultrathin Co film on Si/SiO_2 wafer, instead of using specifically designed catalysts or porous supports, followed by vacuum annealing treatment and C_2H_2 exposure.[22] *In situ* X-ray photoelectron spectroscopy (XPS) indicated that Co−Si reactions at the interface may play an important role in controlling the nanoparticle size distribution, leading to a narrow chirality distribution of SWCNTs in the grown sample. Later on, He, Jiang *et al.* reported the use of epitaxially grown nanocrystals with uniform and well-defined crystalline structures to selectively synthesize SWCNTs.[42] Magnesia (MgO)-supported monometallic Co NPs were prepared by reducing a $Co_xMg_{1-x}O$ solid solution in CO. The dynamics of the formation of Co NPs, monitored by *in situ* transmission electron microscopy (TEM), showed that the epitaxially formed monodispersed Co NPs anchored to the MgO support firmly with little fluctuation during the nanotube growth stage. The lattice-mismatched epitaxy relationship between the Co NPs and the MgO matrix (Figure 4b) may be responsible for the good stability of the Co NPs at high temperature and the uniform size and structure, which are the critical factors to realize the chirality-controlled growth of SWCNTs. Highly selective growth of (6,5) nanotubes with abundance of 53% (Figure 4c) was achieved under optimum growth temperature of 500 °C. This work suggests that lattice-mismatched epitaxially formed catalyst NPs, with uniform size and crystalline structure and good stability at high temperatures, can serve as effective catalysts for the chirality-controlled synthesis of SWCNTs.

Formation of alloys in bimetallic catalyst systems is another practical approach which can increase the stability of metal catalyst NPs and grow CNTs with narrow chirality distributions. A silica-supported bimetallic Fe−Ru catalyst was reported to grow predominant (6,5) SWCNTs under methane CVD.[25] The selectivity toward (6,5) was found to be better at 600 °C, while the selectivity shifted to (7,5), (7,6), and (8,4) when the growth temperature increased to 800 °C. Afterward, a MgO-supported bimetallic Fe−Cu catalyst[23] was also found to be a good catalyst to selectively grow (6,5)-enriched SWCNTs at a low temperature of 600 °C. During the growth stage, Cu was believed to play an important role in inhibiting Fe NPs from aggregating together to form big clusters. So far, for most papers using porous-supported bimetallic catalysts to selectively grow (6,5) SWCNTs, it is essential to keep the CNT growth temperatures low, usually around 600 °C, which may sacrifice nanotube yield and quality. In 2012, Ren *et al.* developed a bimetallic catalyst, silica-supported CoPt, which selectively grew high-quality (6,5)-enriched SWCNTs at a relatively high temperature of 800 °C.[24] The high selectivity at such a high growth temperature was attributed to the high-melting point of CoPt solid alloy, endowing the catalysts good stability at high temperatures. It is expected that by tailoring the catalyst compositions of bimetallic catalysts, considering the large amount of alloys to choose from, improved selectivity and/or selectivity toward more chirality species could be achieved.

Based on all of the progress mentioned above, chiral-selective synthesis was restrained to small-diameter nanotubes only, like (6,5), (7,5), *etc.* Since CNT of each chirality has its own band gap, it is desired to expand chiral selectivity to other chirality species. Chen *et al.* designed a Co-incorporated TUD-1 catalyst (Co-TUD-1) and realized the selective growth of predominant (9,8) SWCNTs, which have relatively large diameters compared to the commonly grown (6,5) SWCNTs.[43] The strong interaction between mesoporous silica support (TUD-1) and Co NPs stabilizes Co NPs and is believed to be responsible for the high selectivity toward (9,8) nanotubes. Later on, a sulfate-promoted $CoSO_4/SiO_2$ catalyst developed by the same group further pushed the selectivity of (9,8) SWCNTs to 33.5% among all SWCNTs.[19] The abundance of (9,8) nanotubes was estimated by optical absorption spectroscopy (Figure 4d). The hydrogen reduction temperature of the catalyst, 540 °C, was found to be essential in order to achieve a good selectivity. Figure 4e shows the relative abundance of various (*n*,*m*) species synthesized from such catalyst at this reduction condition, estimated from micro-Raman, PL excitation (PLE) mapping, and optical absorption spectroscopy. The narrow chirality distribution of SWCNTs may come from the narrow nanoparticle size distribution of the as-formed Co NPs with an average diameter of 1.23 nm, which closely matches the

DOI: 10.1021/acsnano.6b06900
ACS Nano XXXX, XXX, XXX−XXX

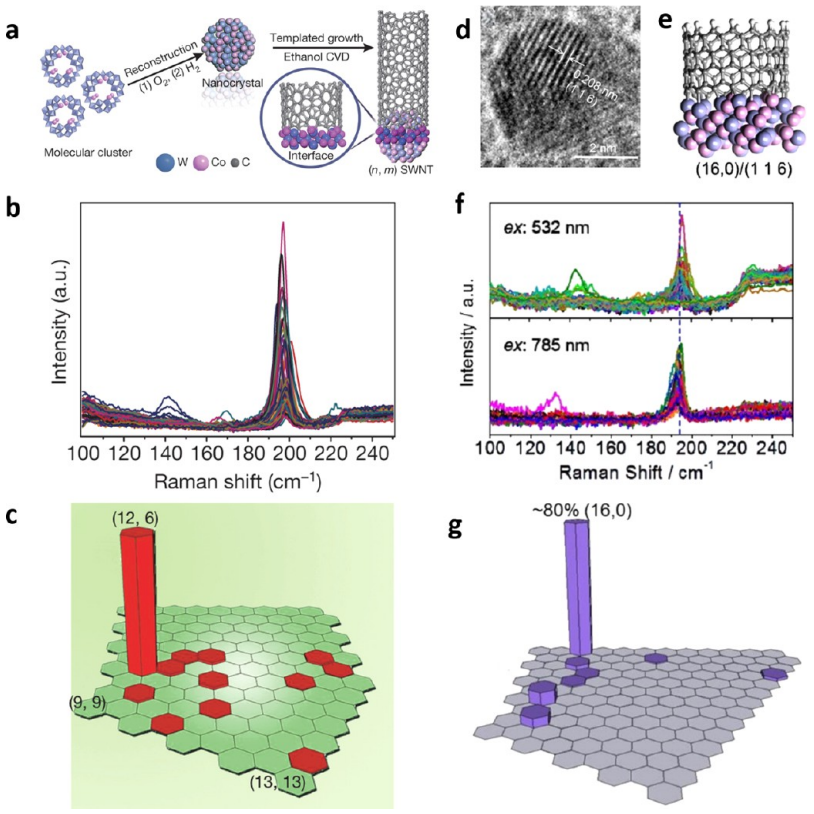

Figure 5. Chirality-selective synthesis of SWCNTs with intermetallic W_6Co_7 solid alloy catalysts.[14,29] (a) Preparation of W−Co nanocrystal catalyst and the templated growth of a SWCNT with specific (*n*,*m*) structure. (b) RBM-region Raman spectra of SWCNTs grown at 1030 °C. (c) Relative abundances of various chiralities denoted in a SWCNT chiral map, quantified by Raman measurements from 3300 nanotubes. (a−c) Reproduced with permission from ref 14. Copyright 2014 Nature Publication Group. (d) HRTEM image of a W_6Co_7 catalyst nanoparticle prepared at 1050 °C. (e) Interface between the (1 1 6) plane of a W_6Co_7 catalyst and a (16,0) nanotube. (f) RBM-region Raman spectra of SWCNTs grown at 1050 °C. (g) Relative abundances of various chirality species quantified from 361 RBMs denoted in a SWCNT chiral map. (d−g) Reproduced with permission from ref 29. Copyright 2015 American Chemical Society.

diameter of (9,8) SWCNTs. The authors attributed the high selectivity to the important roles played by sulfur atoms in forming Co−S compounds and inhibiting aggregation of Co atoms. Overall, $CoSO_4/SiO_2$ catalyst is a good choice to selectively synthesize (9,8) CNTs because it enables chiral selectivity toward a relatively large-diameter nanotube with a satisfying yield. This work indicates that more catalysts with sulfate incorporation are worth further development to achieve chirality-controlled synthesis of SWCNTs with different target chiralities. Recently, a "smart poisoning" approach has been developed by the same group for the selective synthesis of (9,8) SWCNTs.[44] In this approach, Co/SiO_2 catalysts were sulfided in H_2S/H_2 to form Co_9O_8 catalyst nanoparticles, which modulated the selectivity toward (9,8) chirality without sacrificing the growth yield. This sulfidation-based "smart poisoning" concept suggests a promising approach to create catalysts with not only good selectivity but also high activity, aiming for scalable synthesis.

In order to gain a better understanding of the relationship between the chemical composition of catalyst and the chirality distribution of SWCNTs, Sankaran *et al.* compared different Ni_xFe_{1-x} solid alloy NPs with constant sizes.[18] To decouple the influence of catalyst size, fabrication of catalyst NPs with fine-tuned composition at constant NP size was realized by a microplasma-based gas-phase synthesis method. As a result, by solely tuning catalyst composition while keeping all other parameters identical, the authors were able to modify the chirality distribution in the grown SWCNTs.[18] They attributed the change of the chirality distribution of CNTs to the structural change in the catalyst NPs as a result of the change in NP composition, which altered the epitaxial relationship between catalyst NPs and open-ends of CNTs. The intimate relationship between the chirality distributions and the corresponding composition-dependent catalyst structures provides direct experimental support to the epitaxial growth model of CNTs proposed earlier.[45] Meanwhile, the practical methods of precisely fabricating catalyst NPs with tunable compositions and sizes suggest a way to achieve chirality-controlled synthesis of various chirality species *via* the manipulation of catalyst compositions and geometries. This work clearly demonstrates that the chemical composition of catalyst NPs does have a deterministic role on the chirality distribution of thus-grown CNTs and suggests a possible epitaxial relationship between certain chirality CNTs and certain facets of metal catalyst NPs.

The epitaxial growth model suggests that the chirality of SWCNTs can be regulated by the crystal structure of catalysts. This model requests catalyst NPs to be solid and crystalline during CNT growth stage. However, most metals, for example, Fe, Co, and Ni, have relatively low melting points. Furthermore, the melting points of materials would dramatically decrease when the dimension of the material decreases. As a matter of fact, in most cases, the working tiny metal catalyst NPs may stay in a liquid or surface−liquid stage, losing the

DOI: 10.1021/acsnano.6b06900
ACS Nano XXXX, XXX, XXX−XXX

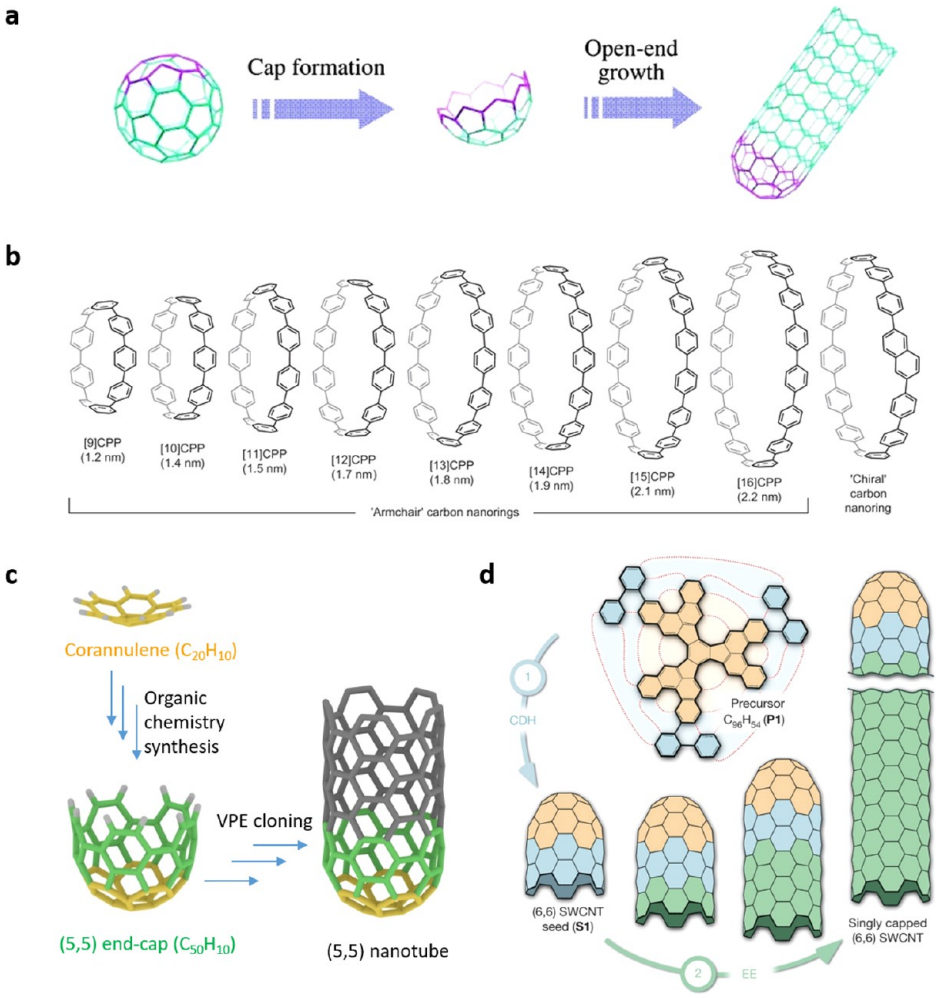

Figure 6. Various carbonaceous molecular precursors for chirality-controlled synthesis of SWCNTs. (a) Schematic illustration of SWCNT growth using fragmented C_{60} as an initiating cap.[58] Reproduced with permission from ref 58. Copyright 2010 American Chemical Society. (b) The structures of some representative carbon nanorings including "armchair" nanorings and "chiral" nanorings.[56] Reproduced with permission from ref 56. Copyright 2013 Nature Publication Group. (c) Structure of the molecular end-caps used for SWCNT growth.[59] Reproduced with permission from ref 59. Copyright 2014 American Chemical Society. (d) Schematic illustration of a two-step bottom-up synthesis of SWCNTs from molecular end-cap precursors.[15] Reproduced with permission from ref 15. Copyright 2014 Nature Publication Group.

controllability to the chirality of as-grown CNTs *via* the above-proposed epitaxial model. In this regard, exploring NPs with exceptional high-melting points is interesting. Noticeably, some nonmetal NPs, like SiO_x, Al_2O_3, SiC, and diamond, have been reported to be able to grow high-quality SWCNTs under suitable conditions in the past few years.[46−50] However, there is no report about chirality-controlled growth of SWCNTs using these nonmetal NP catalysts.

A more recent breakthrough was made by Li *et al.* by developing a tungsten (W)-based bimetallic solid alloy catalyst, W_6Co_7, which has exceptional high-temperature stability.[14] As a result, this catalyst can synthesize (12,6)-enriched SWCNTs with a noticeably high purity of >92% (Figure 5c). Micro-Raman characterization showed dominant RBMs at ~197 cm^{-1} (Figure 5b), and the authors claimed that this peak corresponded to (12,6) SWCNT. This extraordinary high selectivity was attributed to the extremely high-melting point, 2400 °C, of the W_6Co_7 solid alloy catalyst. Thus, the catalyst NPs can remain solid and crystalline at high-growth temperatures, as evidenced by *in situ* TEM study. High-resolution transmission electron microscopy (HRTEM) investigations further showed that the (0 0 12) plane of the W_6Co_7 NPs was the effective plane to nucleate (12,6) nanotube growth due to the perfect structure match between the atomic arrangement on (0 0 12) plane and the open end of a (12,6) nanotube (Figure 5a). This work demonstrates that designing and using high-melting point solid and crystalline NPs with desired facets as catalyst can be a promising approach to achieve chirality control. The interesting point of this work also lies in the fact that nanotubes with (12,6) chirality have a pretty large diameter and moderate chiral angle, and such chirality has been proven to be difficult to be selectively grown previously.

Later on, the same group combined solid alloy catalysts with a suitable kinetic-control approach and achieved selective synthesis of zigzag (16,0) nanotubes,[29] which has been one of the most challenging tasks due to the unfavorable growth kinetics of zigzag nanotubes. X-ray diffraction patterns and a HRTEM image (Figure 5d) indicated plenty of (1 1 6) planes existing in the as-formed W_6Co_7 catalysts. Based on the density functional theory (DFT) simulations, the (1 1 6) plane of W_6Co_7 is a good structure match with the open-end of a (16,0) nanotube (Figure 5e), suggesting that (1 1 6) facet may serve as

DOI: 10.1021/acsnano.6b06900
ACS Nano XXXX, XXX, XXX−XXX

a template for the nucleation of a (16,0) nanotube. In order to shift the selectivity toward the kinetically unfavorable zigzag nanotubes, a higher flow rate of H_2 was used, which has a stronger restraining influence on the growth of nonzigzag nanotubes than that of zigzag nanotubes. Micro-Raman results showed dominant RBM peaks at ~195 cm^{-1} (Figure 5f), assigned to (16,0) chirality, which was then verified by PL and electron diffraction patterns. The abundance of (16,0) nanotubes in the as-grown sample was quantified to be 79.2%, estimated from micro-Raman spectroscopy (Figure 5g). This work proposes a general strategy of combining the catalyst template effect and kinetic control together to realize predominant zigzag nanotube growth. Recently, the same group has further modulated the crystal structure of W_6Co_7 nanocatalysts by introducing water vapor into the reduction and crystallization process of W_6Co_7 and has achieved the selective synthesis of (14,4) SWCNTs with high purity.[51]

In addition to the above success in the use of specially designed metal catalyst NPs toward chirality-selective synthesis of SWCNTs, there are also some reports showing that other growth conditions can also be modified to narrow down SWCNT chirality distributions, despite that the amount of such reports are far less than the amount of catalyst-engineering-based methods. For example, certain selectivity of SWCNTs has been achieved in an aerosol floating catalyst CVD system by introducing a small amount of NH_3 under optimum growth conditions.[27] Narrow chirality distribution centering in a large-diameter (13,12) nanotube has been realized by Kauppinen *et al.*,[27] with over 90% of as-grown nanotubes showing a chiral angle in the range of 20°−30°. Although the role played by NH_3 is still not clear, the authors proposed that the selectivity may come from the etching effect of NH_3, which selectively etched nanotubes with small chiral angles and diameters. Even though the selectivity toward a certain chirality is not very high, it opens up a way to tailor the chirality distributions by introducing an *in situ* etchant like NH_3 to selectively etch some CNT species which are more reactive than others.[52] If this approach can be combined with other chirality control methods, such as catalyst design, porous support, *etc.*, in principle even higher selectivity could be achieved.

Carbonaceous Molecular Precursor Initiated Carbon Nanotube Growth. Recent advances in organic chemistry have enabled synthesis of various carbonaceous molecular precursors, including flat CNT end-cap precursors,[53] 3D CNT end-caps,[54] and carbon nanorings (which are sidewalls of CNTs without caps),[55,56] *etc.*, which have been demonstrated to initiate CNT growth under suitable conditions. The use of pristine C_{60} fullerene for SWCNT growth was reported by Wang *et al.*,[57] but little information was provided about the chirality of thus-grown SWCNTs. At the same time, Liu *et al.* reported an approach of using thermal oxidation to open fullerendione in order to yield hemispherical caps (Figure 6a).[58] Then they used the as-formed caps to initiate SWCNT growth. As a result, the diameter distribution of the as-grown SWCNTs showed a step-like fashion. The lack of perfect control in the structure of hemispherical caps formed by thermal oxidation step makes it challenging to achieve exclusive synthesis of single-chirality CNTs. Later on, Itami *et al.* realized initiation of CNT growth from well-defined carbon nanorings, which can be viewed as sidewall segments of CNTs without caps (Figure 6b).[56] Although the as-grown CNTs had diameters close to the diameter of the nanorings used to initiate CNT growth, unfortunately there was still no successful control over the diameter and chirality of the as-grown nanotubes. An alternative approach of seeded growth was reported by Zhou *et al.*[59] In this work, the authors used 100% pure $C_{50}H_{10}$ molecular seeds synthesized using an organic chemistry approach (Figure 6c), which is the end-cap of a (5,5) nanotube, aiming for chirality-controlled growth of SWCNTs *via* metal-free VPE elongation. High-density, well-aligned CNTs were produced from these seeds on quartz. However, detailed Raman characterization revealed that the formed SWCNTs were not (5,5) chirality. Instead, Raman and electrical measurements indicated that the as-grown nanotubes were nearly pure small-diameter semiconducting nanotubes.[59] The change of CNT chirality during growth from $C_{50}H_{10}$ molecules is believed to originate from the change of the molecular structures at a high-growth temperature of 900 °C. The same may also be true for the chirality-changed growth of SWCNTs from carbon nanorings as discussed above. Further reduction of molecule pretreatment temperatures and CNT growth temperatures may result in chirality-controlled synthesis of (5,5) CNTs from $C_{50}H_{10}$.

At the same time, the use of planar single-crystal metal surface and end-cap precursor for single-chirality SWCNT synthesis with predetermined chirality was reported by Fasel *et al.*[15] To start, a precursor P1 ($C_{96}H_{54}$) was specially designed and synthesized by an organic chemistry method, which yields a (6,6) nanotube seed *via* a surface-catalyzed cyclodehydrogenation (CDH) process (Figure 6d). Then the epitaxial elongation of the seed took place by incorporating a carbon species decomposed by platinum (Pt) surface at a pretty low temperature of 400−500 °C and in a high vacuum of ~10^{-7} mbar. A close-up scanning tunneling microscope (STM) image of a long CNT lying on the substrate unambiguously identified it to be a (6,6) CNT. Furthermore, Raman analysis showed single RBM peaks at 295 cm^{-1}. However, we note that the 532 nm laser used in their study is not in resonance with (6,6) nanotubes. Instead, (9,2) and (10,0) SWCNTs are in good resonance with 532 nm laser, and these two chiralities have RBM peaks very close to 295 cm^{-1}. Moreover, the splitting of G band reported in ref 15 is not consistent with early studies which show that the G-band of armchair metallic CNTs should be a single symmetric peak.[31,60] It is clear that further Raman, absorption, and STM statistic studies are needed to examine whether the as-grown SWCNTs are indeed pure (6,6) chirality in this work. Even though there are still some open issues with the chirality identification, this well-controlled surface-catalyzed synthesis approach is undoubtedly a promising alternative to further develop for chirality-controlled synthesis of SWCNTs. As organic synthesis technology develops, more molecular precursors with more robust structures and higher efficiency may come into reality and realize synthesis of single-chirality CNT products sooner or later. One important advantage of such organic chemistry synthesized molecules is that one can obtain a relatively large quantity of materials, and they have a nominal purity of 100%. In principle, if one can achieve CNT growth using such molecules, it is possible to grow single-chirality CNT species because the seeds/catalysts are identical, while such identical catalysts cannot be achieved so far in either metal NP catalysts or separated CNT templates.

Theoretical Considerations of Chirality-Dependent Carbon Nanotube Growth. In most cases, SWCNTs are produced with a seemingly random chirality distribution, making synthesis of SWCNTs with single chirality challenging. The growth mechanism behind this commonly seen growth

DOI: 10.1021/acsnano.6b06900
ACS Nano XXXX, XXX, XXX−XXX

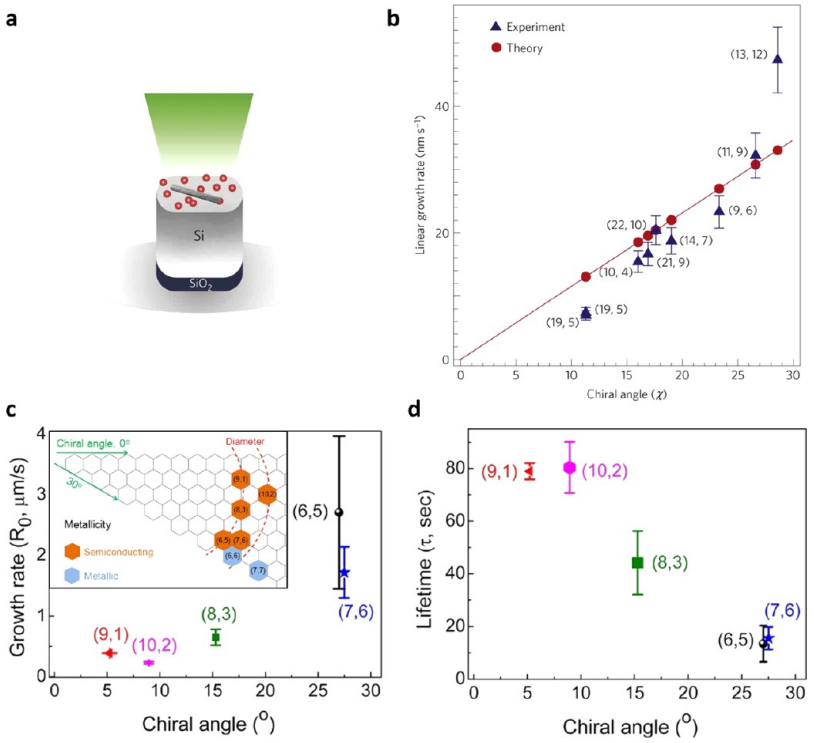

Figure 7. Recent progress in a chirality-dependent growth kinetics study. (a) Schematic diagram showing laser-induced growth of a SWCNT from a catalyst nanoparticle. (b) The linear growth rates (blue triangles) with assigned (*n*,*m*) chiral indices are plotted against the chiral angle χ. The red line represents the growth rate calculated based on the dislocation mechanism of SWCNT growth.[67] (a, b) Reproduced with permission from ref 67. Copyright 2012 Nature Publication Group. (c, d) Chiral-angle dependent growth rate (R_0) and lifetime (τ) of five kinds of semiconducting SWCNTs. The inset of panel c is a chirality map showing the information of the seven chiralities studied.[16] (c, d) Reproduced with permission from ref 16. Copyright 2013 American Chemical Society.

phenomenon has been puzzling to researchers for decades. Yakobson *et al.* proposed a theory viewing any CNT with a chirality of (*n*,*m*) as a zigzag (*n*,0) CNT with an axial *m*-fold screw dislocation.[61] Then they showed that the growth rate of any CNT should be proportional to the magnitude of the Burgers vector of its screw dislocation, thus proportional to the chiral angle of that CNT. Based on this theory, they predicted the dominance of near-armchair nanotubes, which agrees well with experimental results. Later on, metal-free chirality-controlled synthesis of chiral and zigzag nanotubes from carbon nanorings as the growth template was simulated by Morokuma *et al.* using quantum chemical simulations.[62] Similarly, this simulation predicted the same trend that the growth rate of nanotubes would increase with chiral angles. As for the dependence of growth rate on diameter, two different growth mechanisms, C_2H- and C_2H_2-based, led to different results. For the nanotube growth induced by C_2H- radical, the growth rate was independent of the nanotube diameter. In contrast, for the nanotube growth *via* Diels–Alder cyclo-addition, the growth rate was strongly influenced by the nanotube diameter. Given the growth rate is proportional to the chiral angle, it is likely that after a certain growth time, the lengths of CNTs may also be proportional to chiral angles, enabling length to be an important factor for postgrowth selection. Moreover, different carbon species, for example, single carbon atom and C_2 dimer, have been found to interact with growing CNTs following two competitive reaction paths.[63] Specifically, chirality mutation caused by single carbon atom addition, and nanotube elongation induced by C_2 dimer addition.[63] This finding suggests that the concentrations of single carbon atoms and C_2 dimers existing in the reaction environment can affect the chirality selectivity of nanotube growth. In order to better understand the physical mechanism underneath the preference toward chiral CNT instead of achiral species, Yakobson *et al.* combined kinetic growth theory and nanotube/catalyst interface thermodynamics into a single model.[64] Considering kinetic growth theory, CNTs are believed to grow with kinks at the end following a screw dislocation model. Thus, the growth of CNTs with higher chiral angle is favored. On the other hand, based on nanotube/catalyst interface thermodynamics, the nucleation barrier for an achiral nanotube is lower than for a chiral nanotube, favoring growth of achiral species. With these two trends opposite to each other, minimally chiral CNTs become favorable as a "compromise". This result helps explain the predominance of (6,5) nanotubes in the growth products synthesized by various catalytic CVD systems.

Although the screw dislocation theory has done a great job in explaining the high abundance of nanotubes with high chiral angles, the growth rate of zigzag nanotube is ignored in this theory due to the high-energy barrier of adding a new hexagon at the smooth rim of a zigzag nanotube. Despite the small amount of zigzag nanotubes existing in the grown sample, a better understanding of the growth mechanism guiding the zigzag nanotube growth is in need. Ding *et al.* conducted a theoretical study on the growth behavior of zigzag nanotubes through first principle calculations.[65] They found that the growth of zigzag nanotubes followed a stepwise ring-by-ring fashion including two repeatable steps: (1) forming a new hexagon on the smooth rim of a zigzag nanotube, and (2)

DOI: 10.1021/acsnano.6b06900
ACS Nano XXXX, XXX, XXX–XXX

forming a complete hexagon ring with continued growth. As a result, the growth rate was predicted to be 10−100 times slower compared to armchair and chiral nanotubes. Furthermore, the growth rate of a zigzag nanotube was predicted to be proportional to its diameter because a larger diameter nanotube could provide more active nucleation sites on the rim. This theory successfully explained the commonly seen lack of zigzag nanotubes in the grown SWCNTs and completed the growth mechanism of SWCNTs. Another puzzle regarding the chirality-dependent growth rate of CNTs is that double-wall and multiwall CNTs usually have the same lengths for the tubes in different shells, however, it is reasonable to believe that the tubes in different shells possess very diverse chiral angles based on early electron diffraction studies.[66] Then why do CNTs with different chiral angles have the same length after identical growth time? One possible explanation is that there exist strong interactions among CNTs at different shells in a multiwall nanotube, which modulate the growth rates of each shell and eventually lead to the same growth rate and consequently the same length for each shell. Further studies are clearly needed to clarify this point. Overall, with a better understanding of the growth mechanism of SWCNTs, we can gain better control over the chirality distributions of the grown nanotube sample by controlling the growth kinetics.

Chirality-Dependent Growth Kinetics of CNTs. While most researchers focus on controlling the chirality of SWCNTs by controlling the nucleation stage through either catalyst engineering or "growth from template", Maruyama *et al.* studied the growth kinetics of individual SWCNTs and correlated the growth rates of CNTs with their chiralities.[67] Through *in situ* Raman spectroscopy, they have successfully measured the growth rates of individual SWCNTs and correlated the growth rates of SWCNTs to their corresponding chiralities. The setup used in this work was a cold-wall laser-induced CVD as shown in Figure 7a. In this work, the growth rates of SWCNTs were found to be directly proportional to the chiral angles of these SWCNTs (Figure 7b), agreeing well with the theoretical predictions.[61,68] The results in this work suggest a potential route to achieve chiral-selective growth of SWCNTs by careful manipulation of the synthetic strategies based on kinetic control. Later on, our group used the VPE cloning approach[13] to study growth kinetics and termination mechanisms of 7 different single-chirality nanotubes, including (9,1), (6,5), (8,3), (7,6), (10,2), (6,6), and (7,7), ranging from near-zigzag nanotubes to armchair nanotubes.[16] The results showed that as the chiral angles increased, the growth rates also increased (Figure 7c). On the contrary, the active lifetimes of nanotubes decreased with increasing chiral angles (Figure 7d). These experimental results, in good agreement with theoretical predictions,[61,62,64] can guide future growth process designs in order to achieve chirality control from the growth kinetic control perspective.

Growth of Carbon Nanotubes with Controlled Electronic Types (Metallic or Semiconducting). Band gaps of SWCNTs are directly determined by their chirality, classifying nanotubes into two categories based on their electronic conductivities, metallic or semiconducting. The coexistence of both semiconducting and metallic CNTs in most current samples is a big impediment toward the vast applications of SWCNTs in nanoelectronics, macroelectronics, optoelectronics, power cable, *etc.*[69] While ultimate chirality-controlled synthesis of SWCNTs is the top challenge, direct synthesis of SWCNTs with high selectivity toward either semiconducting or metallic is highly desired in many practical applications and may be less difficult than true chirality control. Huge efforts have been devoted to the synthesis of SWCNTs with controlled electronic types over the past two decades. A rational strategy to realize selective synthesis of semiconducting SWCNTs is to selectively etch metallic nanotubes with an *in situ* etchant due to their higher reactivity compared to semiconducting nanotubes. Oxygen was reported by Cheng, Kauppinen *et al.* to be an effective *in situ* etchant to selectively etch metallic species during SWCNT synthesis by floating catalyst CVD.[70,71] Later on, Liu *et al.* found water vapor to be an alternative effective *in situ* etchant for metallic nanotube etching and realized selectivity of semiconducting nanotubes as high as 97%.[72] Afterward, the selectivity of metallic nanotube etching was found to be diameter dependent on the quartz substrate.[73] Hence, better selectivity of metallic nanotube etching can be achieved by narrowing the diameter distribution into a small and optimum range. To realize a narrower diameter distribution of the grown SWCNTs, bimetallic solid alloy catalyst Fe−W nanoclusters, which are stable at high temperature, were utilized under optimum etchant concentration. Electrical measurements conducted on individual SWCNTs indicated the purity of semiconducting species was around 95%. This work offers a good strategy of combining diameter control with *in situ* etchant to realize high selectivity toward semiconducting nanotubes. An alternative approach to selectively synthesize semiconducting nanotubes is to use ceria as the catalyst support, which can provide an oxidative environment during the nucleation and growth processes to inhibit the formation of metallic species.[74] Moreover, different carbon sources have been investigated and found to be related to the abundance of semiconducting species in the grown sample. Liu *et al.* reported that the introduction of methanol in the ethanol CVD growth process could lead to selectivity as high as 95% on a quartz substrate.[75] Later on, Zhou *et al.* have found that isopropyl alcohol (IPA) is an effective carbon source to produce semiconducting-enriched SWCNTs with purity ~90%,[21] due to the suitable amount of water vapor present in the IPA CVD environment. Recently, oxygen-deficient TiO_2 NPs, with the ability of generating oxygen vacancies, were reported to selectively grow semiconducting nanotubes with a percentage of over 95%.[76] The selectivity was attributed to the oxygen vacancies generated by the catalyst which made the formation energy of semiconducting nanotubes lower than that of metallic nanotubes. Another recent breakthrough has been made by Cheng *et al.* by using specially designed acorn-like, partially carbon-coated Co nanoparticle catalysts.[77] Combining with *in situ* etching of metallic nanotubes, they achieved selective synthesis of semiconducting nanotubes with a purity higher than 95% and with a narrow band gap distribution (band gap difference as small as 0.08 eV). To sum up, all of the approaches mentioned above are effective to grow semiconducting-enriched SWCNT products by either selectively removing the metallic species or directly inhibiting the formation of metallic nanotubes.

Although metallic nanotubes are usually not wanted for applications in digital circuits, metallic nanotubes with high purity are actually highly desired in other applications, like power cables, which require high electrical conductivities. Overall, there were very few reports on the selective growth of metallic-enriched SWCNTs. Harutyunyan *et al.* realized predominant growth of metallic nanotubes with a percentage as high as 91% by optimizing the noble gas ambient for catalyst

DOI: 10.1021/acsnano.6b06900
ACS Nano XXXX, XXX, XXX−XXX

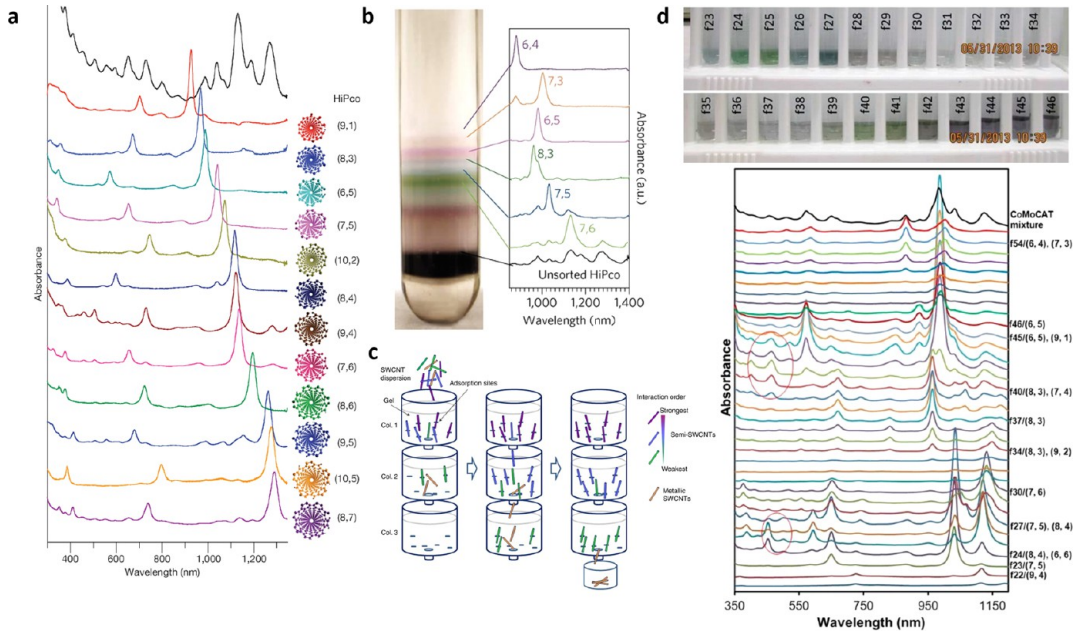

Figure 8. Single-chirality SWCNTs separation methods. (a) IEX separated 12 major semiconducting single-chirality DNA-wrapped SWCNTs.[30] Reproduced with permission from ref 30. Copyright 2009 Nature Publication Group. (b) HiPco SWCNTs sorted by nonlinear DGU and the absorption spectra of the colored layers showing the single-chirality enrichment.[83] Reproduced with permission from ref 83. Copyright 2010 Nature Publication Group. (c) A schematic illustrating the single-surfactant multicolumn gel chromatography sorting procedures.[84] Reproduced with permission from ref 84. Copyright 2011 Nature Publication Group. (d) Photographs of collected fractions of single-chirality SWCNTs separated by countercurrent chromatography (upper panel) and their corresponding UV−vis-NIR absorption spectra (lower panel).[92] Reproduced with permission from ref 92. Copyright 2014 American Chemical Society.

annealing and the H_2/H_2O ratio.[28] *In situ* TEM results indicated that the catalyst annealing conditions could affect the catalyst morphology and thus affect the nucleation of carbon nanotubes. With more efforts devoted to further improving the purity of metallic nanotubes, metallic SWCNTs with high electrical conductivity but low mass can be ideal candidates for many applications, such as power cables, transparent conductive films, *etc.*

POSTSYNTHESIS PURIFICATION OF SINGLE-CHIRALITY CARBON NANOTUBES

In addition to direct controlled synthesis, postsynthesis separation is another effective way to obtain single-chirality SWCNTs. Many powerful methods for chirality separation have been demonstrated in the past decade or so. In 2004, Zheng *et al.* reported the successful enrichment of (6,5) nanotubes *via* ion-exchange chromatography (IEX) separation of DNA-wrapped SWCNTs.[78] In 2007, Zheng *et al.* achieved purification of (6,5), (6,4), and (9,1) nanotubes by conducting size exclusion chromatography (SEC) separation first to narrow the nanotube length distribution, followed by IEX.[79] Later, hundreds of single-stranded DNA (ss-DNA) sequences were tested to identify SWCNT recognition sequences, which resulted in the purification of all 12 major semiconducting single-chirality SWCNTs from a synthetic mixture (Figure 8a).[30] Through single-point scanning mutation and sequence motif variation of previously identified ss-DNA sequences for semiconducting tubes, recognition sequences for the metallic armchair (6,6) and (7,7) have also been identified, resulting in the purification of the corresponding SWCNT species.[31] The mechanism of the IEX separation is becoming clearer after years of investigations. DNA−SWCNT interaction and the resulting hybrid structure are dependent on both the DNA sequence and the chirality of SWCNT. Some hybrids have well-ordered DNA folding structure when the DNA-sequence is properly chosen. IEX is basically a selection method that picks out ordered DNA-SWCNT hybrids that show minimum electrostatic and electrodynamic interactions with the ion-exchange resin. This selection process and the molecular recognition involved led to single-chirality SWCNTs with such high purity levels that few other methods can offer. However, the cost of DNA should be taken into consideration concerning scaling-up of the process.

Another approach is to exploit differences in the buoyant densities among SWCNTs of different structures. In a density gradient, the balance between buoyant force and centrifugal force results in SWCNTs with different buoyant densities to locate in their respective layers in the gradient, and therefore separation can be achieved. Hersam's group developed a density gradient ultracentrifugation (DGU) approach to separate surfactant-coated SWCNTs according to their electronic structures and diameters.[80] High-purity (6,5) SWCNT samples were produced *via* orthogonal iterative DGU.[81] When a chiral surfactant sodium cholate was used for SWCNT dispersion, enrichment of left- and right-handed (6,5) SWCNTs were also demonstrated.[82] A significant step forward was the development by Weisman's group of nonlinear DGU, which resulted in the purification of 10 semiconducting single-chirality SWCNTs and enantiomerically enriched fractions of 7 pairs of (n,m) species.[83] Figure 8b illustrates an image of sorted layers obtained by a nonlinear DGU separation of HiPco SWCNTs and absorption spectra of the separated layers showing single-chirality enrichment.

Gel chromatography has also been adopted for single-chirality purification of surfactant-dispersed SWCNTs.[84,85] In this approach, allyl dextran-based polymer beads are employed

DOI: 10.1021/acsnano.6b06900
ACS Nano XXXX, XXX, XXX−XXX

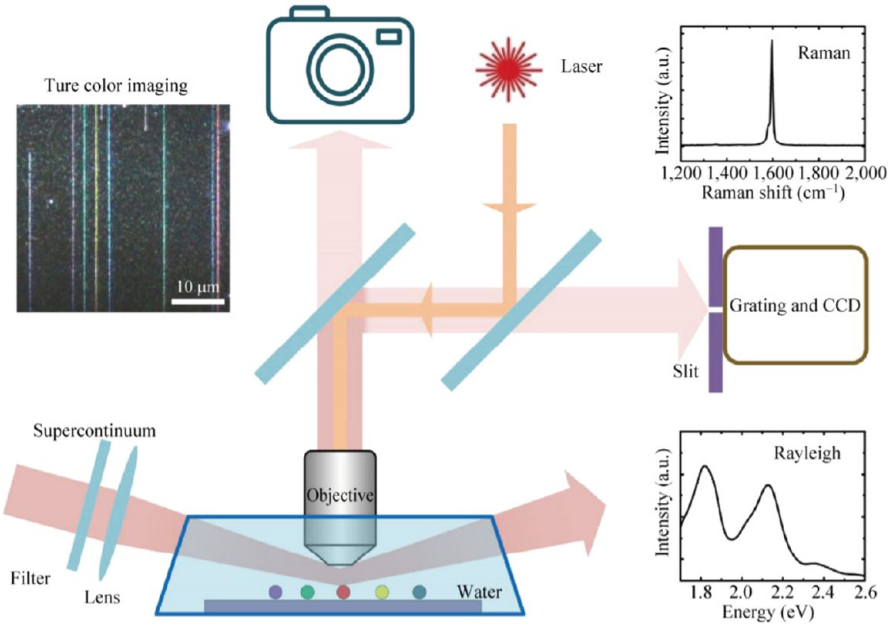

Figure 9. High-throughput, true-color, and real-time imaging and chirality characterization of surface-grown SWCNTs using a RIAS method.[106] Reproduced with permission from ref 106. Copyright 2015 Springer.

as the stationary phase. Adsorption of surfactant-dispersed SWCNTs on the stationary phase is highly sensitive to the structure of SWCNTs and can be tuned by the choice of surfactant used for SWCNT coating and for the mobile phase. Temperature also has a strong effect on the adsorption. By modulating the adsorption and desorption processes *via* control of surfactant and temperature, Kataura's group showed that 13 chiralities of SWCNTs were separated with purity up to 93% in a large scale (Figure 8c).[84] Subsequent work from the same group demonstrated that simultaneous single-chirality and enantiomer purification of many semiconducting SWCNTs have been achieved.[86,87] Recently, this method has been further optimized to realize milligram-scale separation of high-purity single-chiraltiy SWCNTs.[88]

Recently, Zheng *et al.* introduced the aqueous two-phase (ATP) separation technique, a technique widely used for biochemical separations, for SWCNT separation.[89] A polymer ATP system exploits the polymer phase separation phenomenon to create two separate but permeable water phases of slightly different structures.[90,91] As a result, the hydration energy of a solute is rescaled differently in the two phases, leading to uneven solute distribution. This can be exploited for separation. Both surfactant-dispersed and DNA-dispersed SWCNTs can be separated by ATP to achieve single-chirality SWCNT purification.[92−96] Figure 8d shows that an automated ATP process can be performed to achieve single-chirality purification in a single run. Overall, compared with other existing CNT separation methods, the ATP separation method is quick, low-cost, and feasible to scale up.

CHIRALITY CHARACTERIZATION

How to measure the chirality of a nanotube and the population of each chirality in a SWCNT sample is of equal importance with the chirality-controlled preparation of SWCNTs. There are two categories of techniques to measure the chirality of SWCNTs, *i.e.*, direct-imaging-based techniques and spectroscopy-based techniques. Direct-imaging methods include atomic-resolution AFM, STM, and TEM.[15,97] Spectroscopy methods mainly include optical absorption spectroscopy, PL spectroscopy, Raman scattering spectroscopy, Rayleigh scattering spectroscopy, electron diffraction, *etc.*[7,52,98−104] In general, imaging-based methods can provide direct and accurate information on the chirality of SWCNTs, and *via* large numbers of statistic studies, in principle, these methods could provide convincing and quantitative information about the population of each chirality in a SWCNT ensemble. However, there are noticeable drawbacks with these imaging methods, such as, long operation time, high requirement to the instrument, and special sample preparation procedures. In most studies, spectroscopy-based methods are frequently used with advantages of, for instance, short operation time, relatively easy sample preparation procedures, and general availability of the instrument like Raman microscopy and absorption spectrometer in many laboratories.

Currently, researchers can achieve chirality-controlled or chirality-enriched growth of SWCNTs in both bulk growth and surface growth forms. It is now not challenging to characterize the chirality distribution of SWCNTs in a sample. However, how to obtain quantitative information about the population of each chirality in a SWCNT ensemble in a relatively fast and convincing way is difficult. For bulk nanotubes grown with methods such as CVD processes using porous substrates or high-surface-area substrates, and floating catalyst CVD process, since one can obtain relatively large quantity of nanotubes, spectroscopy methods are widely used to determine the structures and properties of nanotubes grown with such methods. Usually, SWCNTs would be dispersed in aqueous or organic media with the assistance of surfactants, DNA, or polymers, to form individually dispersed nanotube dispersions. Then, one can perform optical absorption or PL measurements on such nanotube solutions and obtain semiquantitative information about the population of each chirality in a nanotube sample. It is worth pointing out that PL measurements can only detect semiconducting SWCNTs, while optical absorption measurements work for both semiconducting and metallic SWCNTs. In addition, one should note that these

DOI: 10.1021/acsnano.6b06900
ACS Nano XXXX, XXX, XXX−XXX

methods work well for relatively small-diameter SWCNTs, while for large-diameter SWCNTs, there are some uncertainties in chirality identification. First, water is the most frequently used solvent to disperse SWCNTs, and due to the fact that water itself absorbs light strongly for wavelength >∼1400 nm, other solvents should be considered if the interested nanotube absorptions are in the range above 1400 nm. The solvents of consideration can be heavy water (deuterium oxide, D_2O, which can extend the spectra to ∼1600 nm),[24] or some organic solvents such as toluene.[105] Second, for large-diameter SWCNTs, the number of combinations of (n,m) which have similar E_{ii} transition energies increases significantly and becomes much greater than that of small-diameter SWCNTs. Therefore, careful analysis should be given to assign the chirality of large-diameter SWCNTs based on the optical absorption or PL measurements. Raman spectroscopy is another powerful method to measure the chirality and quality of SWCNTs in a fast and nondestructive way. Although Raman spectroscopy can tell the existence or absence of SWCNTs of certain chirality easily, it is very challenging to obtain quantitative information about the population of each chirality since the Raman intensity of RBM peaks is related to many other factors besides the amount of nanotubes.

On the other hand, for surface-grown SWCNTs, usually the amount of SWCNTs is low to conduct optical absorption or PL measurements to obtain quantitative information about the population of each chirality. In spite of the difficulty, the use of optical absorption, PL, Raman scattering, or Rayleigh scattering to measure the chirality of individual SWCNTs on substrates have been realized. However, it is anticipated that a large amount of spectra needs to be taken to obtain quantitative information of each chirality nanotube, which would be time-consuming. Unlike bulk SWCNT samples, so far, it is still challenging to obtain convincing information about the chirality population in surface-grown SWCNTs. One solution to this problem is to combine the direct imaging method with spectroscopy methods together, which may greatly speed up the characterization process and enable high-throughput chirality characterization of surface-grown SWCNTs. In a very recent study, Jiang *et al.* have developed a powerful Rayleigh-imaging-assisted spectroscopy (RIAS) method which can do true-color real-time imaging and spectroscopy of surface-grown SWCNTs without the need of decorating SWCNTs with small solid particles or water droplets (Figure 9).[106] The authors have managed to significantly improve the Rayleigh scattering process *via* an interface dipole enhancement effect,[107] which allows for the direct imaging of SWCNTs *via* Rayleigh scattering. There are several innovations in this method. First, the authors used supercontinuum (SC) white laser, which has a much higher intensity than a normal light source, as the incident light during Rayleigh imaging. Second, a suitable medium with a matching refractive index with the substrates where nanotubes lie on was used to eliminate light scattering from the substrate and, consequently, to improve the visibility and image quality of SWCNTs during Rayleigh scattering based imaging. Third, this Rayleigh imaging system was integrated with resonant Raman spectroscopy and Rayleigh spectroscopy and allows for the imaging and spectroscopy analysis. As a result, SWCNTs with different chiralities show different colors during imaging, which provides an overview of information about the structure heterogeneity of the samples over a large area of 100 × 100 μm. Later, since the SWCNTs can be seen under optical microscopy, Raman and Rayleigh spectra can be easily collected for subsequent chirality analysis. This method allows for high-throughput imaging and measuring the chirality distribution of surface-grown, low density SWCNTs, and we think this method could be very helpful to evaluate the success of chirality-controlled SWCNT growth in surface-grown samples, which was difficult previously.

APPLICATIONS OF CHIRALITY-PURE CARBON NANOTUBES

The driving forces for the chirality-controlled preparation of SWCNTs have many aspects, including the use of chirality-pure SWCNTs for fundamental studies on chirality-dependent properties of SWCNTs and applications of SWCNTs with pure chirality and well-controlled properties in different research areas.[12,108,109] In recent years, with the availability of single-chirality or highly chirality-enriched SWCNT samples, researchers have conducted many fundamental and applied studies based on these chirality-pure SWCNT samples.

Fundamental Research. There is a huge amount of theoretical literature predicating that many properties of SWCNTs are chirality-dependent, such as electronic band structure, optical properties, thermal conductance, chemical reactivity, optical absorption/emission coefficients, *etc.*[110−113] The penetration of CNTs into cell membranes is also chirality-dependent based on theoretical calculations.[114] A previous strategy to study chirality-dependent properties of nanotubes was randomly picking up SWCNTs, measuring their properties, and then determining the chirality of the studied SWCNTs either *in situ* or *ex situ*. For example, the chirality-dependent electronic structure of SWCNTs, which is one of the most important features of such chirality-dependent properties of SWCNTs, was verified experimentally in 1998 *via* STM studies of randomly picked SWCNTs, and the results confirmed early theoretical calculations.[115,116] In a later study, Liu *et al.* performed *in situ* electron diffraction studies and transport measurements to correlate the transport properties of double-wall CNTs with the chirality of both outer and inner tubes.[100] In another study, Cheng, Kauppinen *et al.* used electron diffraction and studied chirality-dependent reactivity of SWCNTs to oxygen and found that metallic SWCNTs are more reactive than semiconducting ones when they have similar diameters,[52] which sheds light on the mechanism of selective growth of semiconducting SWCNTs in oxidative environments as reported by many groups.[21,71,75,117] However, it is difficult to test many other theoretical predications experimentally, because of the inability to select SWCNTs with a particular chirality or the lack of a reasonable amount of SWCNTs with uniform chirality. For example, it is known that for SWCNTs with very small diameters, there should be some deviations from the tight-binding theory based calculations of the chirality-dependent band structures, because strains play important roles in such small-diameter SWCNTs. Recent DFT calculations have predicted that (5,0) CNTs actually should be a metal with a zero band gap,[118] which contradicts the commonly accepted view that a (n,m) tube should be a semiconductor if $(n - m)$ is not an integer multiple of 3. However, this prediction[118] cannot be tested experimentally so far, because it is hard to selectively synthesize, separate, or pick up a (5, 0) CNT for such a particular study.

With recent successes in obtaining single-chirality or highly chirality-enriched nanotube samples, by now researchers have conducted several experimental studies to examine chirality-dependent properties of SWCNTs. For example, with the

DOI: 10.1021/acsnano.6b06900
ACS Nano XXXX, XXX, XXX−XXX

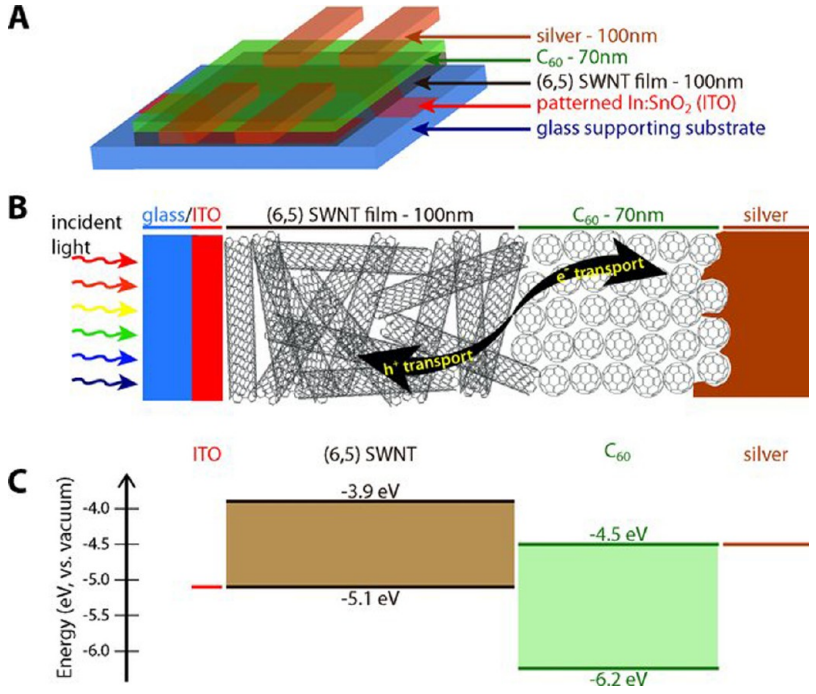

Figure 10. Solar cells using (6,5) SWCNT as the hole transport layer and the IR absorption layer. The electron transport layer was fullerene.[123] (a, b) Polymer-free photovoltaic device which contains glass/ITO hole-collection electrode, (6,5) SWCNT film as the hole transport layer, C_{60} film as the electron transport layer, and silver as the electron collection electrode. (c) Energy diagram of the device with a type II heterojunction due to the relative position of the conduction and valence energy levels of (6,5) chirality SWCNT and fullerene C_{60}. Reproduced with permission from ref 123. Copyright 2012 Wiley-VCH Verlag GmbH & Co.

ability to separate single-chirality SWCNTs from the DNA-based recognition method, Dai, Zheng *et al.* have fabricated FETs using enriched (10,5) SWCNTs.[119] The results indicate that transistors based on (10,5) SWCNTs, which have a relatively large diameter of 1.03 nm, have a larger on-state current compared to transistors made from small-diameter (0.8−0.9 nm) SWCNTs. This is due to the fact that large-diameter SWCNTs can deliver a large current, and also it is easy to form low-resistance contacts for large-diameter SWCNTs.[119] In addition, by taking advantage of DNA-based SWCNT recognition and separation techniques, Doorn, Telg *et al.* have measured Raman spectra of 14 kinds of SWCNTs which were highly enriched with different chiralities.[120] They further established the relationships between chirality and the tangential G-mode features of these SWCNTs. As a result, researchers can now use not only the RBM features but also the G-modes from the Raman spectra to determine the chirality of SWCNTs, which have expanded the usage of Raman spectroscopy in nanotube research. The availability of pure armchair (*n*,*n*) SWCNTs, which are true metallic species with massless carriers, allows experimental studies of a lot of interesting physics of armchair nanotubes including electron−electron interactions, one-dimensional (1D) excitons and photons, and Tomonaga−Luttinger liquids, *etc.*[31,60,121] For example, it has been shown that armchair (6,6) and (7,7) SWCNTs have a single and symmetric tangential G-mode in Raman spectra,[31] which was not reported in previous theoretical studies. In turn, such features of G-mode for armchair SWCNTs may also serve as an important criterion to evaluate whether an as-grown SWCNT sample is enriched with an armchair tube.[15]

Energy Applications. Our world is facing a global energy challenge as the society's demand for energy increases dramatically. Using photovoltaic devices for solar energy harvesting is an important way to potentially solve the energy crisis. CNTs possess several noticeable advantages that make them interesting for use as solar cell components, including high charge mobility, strong absorption of visible to near-infrared (IR) light, large intratube exciton diffusion length, good stability in air, and solution-compatible processing.[122] The incorporation of SWCNTs into solar cells as near-IR absorbers has shown great promise since SWCNTs can absorb light in such an IR regime efficiently. For solar cell devices, or more generally many other devices which involve charge transfer at the interface of materials, energy band alignment among different functional components is critical to achieve good light absorption, electron and hole transfer, and the overall solar energy conversion efficiency. SWCNT-fullerene as donor−acceptor pairs for solar cells has been extensively explored, and there are several possible ways to further optimize the device performance, including energy band alignment between these two materials, interface, traps, light absorption, *etc.* In a recent study, Strano *et al.* used (6,5) chirality-enriched SWCNTs and fabricated a polymer-free solar cell (Figure 10).[123] The unique point of (6,5) SWCNT is that, due to its specific energy levels, it can form a type II heterojunction with fullerene and thus facilitate a lower barrier transport path for holes. As a comparison, nanotubes with a 20% impurity of (6,4) chirality resulted in a 30× decrease in power conversion efficiency (PCE). The reduction in PCE was caused by the lack of well-defined band alignment between the SWCNT film and fullerene C_{60}. Due to the presence of impure SWCNTs, which leads to nonuniform band gaps and energy levels of SWCNTs, electrons and holes can be trapped within the SWCNT film and facilitate exciton recombination, which is harmful for achieving a high PCE in photovoltaic devices. The

DOI: 10.1021/acsnano.6b06900
ACS Nano XXXX, XXX, XXX−XXX

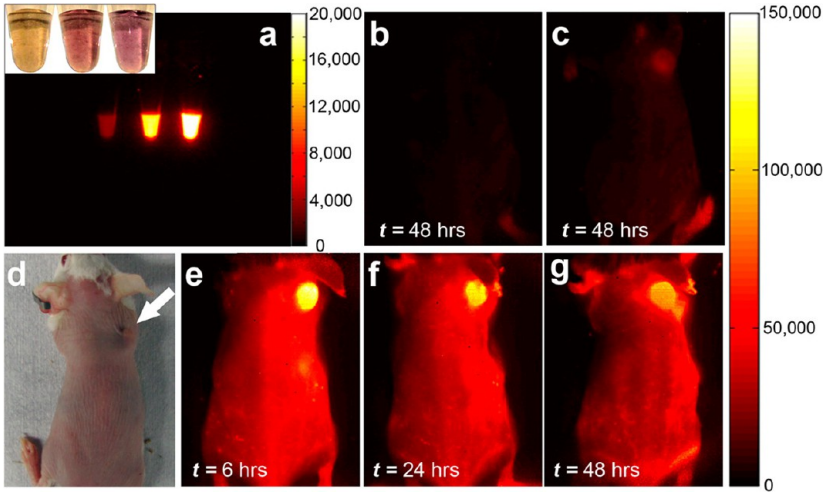

Figure 11. Biological imaging using chirality-enriched SWCNTs.[132] (a) Optical image (upper left) and PL image of unsorted SWCNTs (left), (6,5)-enriched SWCNTs (middle), and (6,5)-enriched SWCNTs with a higher purity than the middle one (right). The concentrations of the SWCNTs are the same. (b, c) and (e–g) Near-IR II fluorescence images of tumor-bearing mouse injected with PBS control (no signal), unsorted SWCNTs (weak signal), and (6,5) chirality-enriched SWCNTs (very strong signal). (d) Optical image of a mouse bearing tumor at its right shoulder. The right vertical bar indicates the intensity of the PL at near 900–1400 nm regime after excitation at a laser at 808 nm. Reproduced with permission from ref 132. Copyright 2013 American Chemical Society.

importance of chirality selection on the charge transfer between SWCNT and fullerene in solar cells was also reported in another study by Isborn, Tung *et al.*, by fabricating and comparing the performance of solar cells comprised of (9,7), (7,6), or (6,5) SWCNTs as the active components.[124] However, the PCE was not high by using single-chirality-enriched SWCNTs, due to the fact that (6,5) SWCNTs can only absorb few portions of solar light, which are in resonance with the nanotube's E_{ii} energies.[125] Nevertheless, the use of single-chirality SWCNTs provides a much simpler device design than a mixture of SWCNTs[126] to study the limiting factors which lead to the low PCE in carbon-based solar cells. In a more recent publication, the diameter limit of SWCNTs to be used efficiently for polymer-free SWCNT-fullerene solar cells has been determined by Flavel *et al.*, which offers guidance in the chirality selection for building high performance SWCNT-fullerene solar cells.[127] More generally speaking, for any devices where charge transport is involved, the rational selection and on-purpose growth of SWCNTs with desired energy levels could be beneficial to the device performance because energy band alignment is important for all such devices, including metal contacts to SWCNT field-effect transistors, hydrogen evolution, carbon dioxide reduction, nanotube-nanomaterial junction devices, *etc.*[128−131]

Biological Applications. SWCNTs hold great potential for biological and medical applications including biological imaging, photothermal therapy, drug delivery, *etc.*[132−135] SWCNTs can absorb light in visible to near-IR regimes, which can be used for photothermal therapy. In addition, semiconducting SWCNTs have an intrinsic band gap PL with a wavelength at near-IR regime, which is of great interest for biological imaging. For biomedical imaging applications, fluorescent species that can emit light in near-IR regime are in high demand, because biological systems do not absorb near-IR light strongly and the wavelength of 700–1700 nm is a biological transparent window. More importantly, the scattering of light by biological tissues is related to the wavelength of the light with a relationship of scattering $\propto \lambda^{-\alpha}$. Therefore, the longer the wavelength of the light is, the smaller the scattering and the deeper penetration of the light into the tissues, and consequently more suitable for imaging deep inside the body.[132,133] The 1D nature of SWCNTs makes them have absorption and emission at well-defined energies (E_{ii}) corresponding to the Van Hove singularities, and the energy of the E_{ii} transitions can be further tuned by tuning the chirality of SWCNTs. The use of as-grown SWCNTs with random chiralities for biological imaging has been studied extensively.[134] However, due to the 1D structure of the nanotubes, only a very small portion of SWCNTs (for example, <9% for HiPco samples) that are in resonance with the incident laser can emit light,[7,132] while the rest of SWCNTs are silent and do not contribute to the imaging. In recent studies, Dai *et al.* have combined recent advances on nanotube chirality separation techniques with *in vivo* biological imaging and have significantly improved the detection sensitivity and reduced the required nanotube dosage during biological imaging. In one study, by tuning the composition of surfactants, they managed to obtain (12,1) and (11,3) chirality-enriched SWCNTs using the gel filtration method.[133] These two SWCNT chirality species have very similar E_{11} (~803 nm for (12,1) chirality and ~798 nm for (11,3) chirality) and E_{22} (~1171 nm for (12,1) chirality and ~1197 nm for (11,3) chirality) energies, and consequently, they can be excited by a single wavelength laser (808 nm) and both can have strong PL at ~1200 nm. The results show that compared with as-grown HiPco nanotubes with many chiralities, the separated, (12,1) and (11,3) chirality-enriched SWCNTs have a 5× stronger PL, and as a result, a 6-fold lower injection dosage is needed to achieve a good biological imaging. Considering the facts that the purities of (12,1) and (11,3) SWCNTs are still not very high judging from the optical absorption spectra shown in the paper, and those two SWCNTs do not emit light at exactly the same wavelength, further optimization by using single-chirality SWCNTs with even higher purity could further improve the performance of nanotubes for biological imaging. In a follow-up study, the same group used DGU-separated, highly enriched single-chirality (6,5) SWCNTs for dual imaging and photothermal therapy purposes with a lower dosage of SWCNTs.[132] It can be clearly

DOI: 10.1021/acsnano.6b06900
ACS Nano XXXX, XXX, XXX–XXX

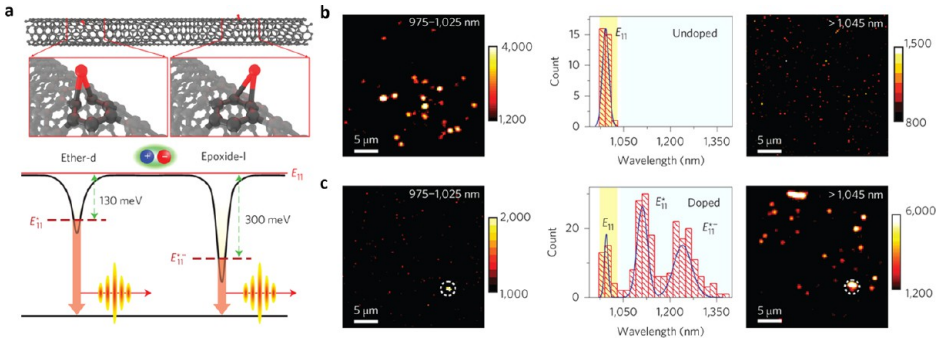

Figure 12. Single photon sources made of solitary oxygen-doped (6,5) SWCNTs.[138] (a) Schemes showing the formation of ether-d and epoxide-l groups on a SWCNT, which leads to the creation of deep trap states located 130 meV (E_{11}*) and 300 meV (E_{11}*$^{-}$) below the E_{11} state of SWCNTs. (b, c) 2D PL intensity maps of undoped (6,5) (b) and solitary oxygen doped (6,5) SWCNTs. Left: Signals collected in the 975−1025 nm emission range. Middle: Histogram of the wavelength of the emitted light. Right: Signals collected in >1045 nm range. Reproduced with permission from ref 138. Copyright 2015 Nature Publication Group.

discerned that (6,5)-enriched SWCNTs possess a much brighter PL than the unsorted raw HiPco samples which have a mixture of many chiralities (Figure 11a). In addition, by irradiating the nanotube solution under a 980 nm laser, the (6,5)-enriched sample underwent a greater temperature increase than the unsorted one, due to resonant absorption and consequently highly efficient heating of (6,5) SWCNTs by a 980 nm laser which is in resonance with the E_{11} of (6,5) SWCNTs. More specifically, compared with unsorted HiPco SWCNTs with random chirality distribution, the (6,5)-enriched SWCNTs are 6-fold brighter in PL, which led to clear tumor imaging, and reached the required photothermal tumor ablation temperature with a more than 10-fold lower injected dosage. The intravenous injection concentration of 0.254 mg/kg of SWCNTs is the lowest reported dosage for nanomaterial-based *in vivo* therapeutics and can deliver clear imaging (Figure 11). Concerning the toxicity and biocompatibility issues of nanomaterials, the low dosage is a much appreciated advantage. These results clearly demonstrated the powerfulness of chirality-enriched samples on the performance of nanotube probes for biological imaging and photothermal therapy applications. Moreover, the unique electronic and optical properties of SWCNTs also make it rather feasible to do biological imaging at different wavelengths of interest, *via* choosing nanotubes with different chiralities. For example, in another study, Dai *et al.* have demonstrated the separation of (6,4)-enriched SWCNTs (>99% purity) by tuning the PH during DGU separation process and the use of such ultrahigh-purity (6,4) SWCNTs for NIR-I biological imaging.[135] The unique point of (6,4) SWCNT is that this nanotube has an E_{22} energy of ∼1.42 eV (∼873 nm), and therefore, an ordinary silicon detector, instead of an expensive InGaAs detector, was used to detect the emitted light since the silicon detector still has a good efficiency at this wavelength. This could reduce the cost of imaging greatly and make it more practical for use in a clinical environment. As mentioned above, by increasing the wavelength during imaging, the scattering of light by biological tissues is much weaker, thus offering a much deeper penetration depth, and the interference with autofluorescence is also reduced. These features call for the preparation of large-diameter single-chirality SWCNTs for biological imaging at an even longer wavelength, for example, >1400 nm.

Single Photon Sources. Single photon source is a light source that emits light as single photons and is an important component in technologies such as quantum key distribution and photonic quantum information processing. Crystal structure imperfections in solids often act as efficient carrier trapping centers, which, when suitably isolated, can be harvested as sources of single photon emission. Some of the well-known examples include semiconducting heterostructures and colored centers in diamond (nitrogen vacancy).[136] The use of CNTs and monolayer two-dimensional (2D) semiconductors as single photon sources has also been reported in the past years. For example, in some recent studies, researchers have shown that monolayer WSe_2 can be a single photon source that emits light in the visible light range.[137] On the other hand, single photon sources that are capable of emitting light in the telecom wavelength range of 1300−1550 nm and at room temperature are particularly important to the realization of quantum optical applications. In a recent study, Htoon, Doorn *et al.* have developed a technique to dope chirality-pure (6,5) SWCNTs with solitary oxygen and realized room-temperature, fluctuation-free, and stable single photon sources working at a near-IR regime of 1100−1300 nm (Figure 12).[138] The authors used single-chirality (6,5) SWCNTs that were separated using an ATP method and deposited these (6,5) SWCNTs on a silicon substrate coated with Au and SiO_2 film. Later, another thin layer of SiO_2 (10 nm) was deposited on top of the SWCNTs using e-beam evaporation to encapsulate the nanotubes. They found that such thin SiO_2 layers can dope SWCNTs at a low concentration to form solitary oxygen dopants. Such solitary oxygen dopants, which form spatially localized either ether-d or epoxide-l functional groups on the sidewall of (6,5) SWCNTs, can create optical transition states that are pinned to deep trap states located ∼130 meV (E_{11}*) and 300 meV (E_{11}*$^{-}$) below the E_{11} band-edge of SWCNTs (Figure 12a). Since the concentration of oxygen dopants is very low, they can form isolated trapping centers in the (6,5) SWCNTs and realize strong exciton localization, which is critical for single photon emission. Figure 12b shows undoped (6,5) SWCNTs which emit light at 975−1025 nm, close to the E_{11} transition energy of (6,5) SWCNTs (∼975 nm). Note that there is no emission at >1045 nm wavelength for undoped (6,5) SWCNTs, as seen from the middle and right panels of Figure 12b. In contrast, for the solitary-oxygen-doped (6,5) SWCNTs, they observed strong emission centered at 1120 and 1250 nm (Figure 12c), exactly 130 and 300 meV below the E_{11} transitions of undoped (6,5) SWCNTs. These results indicate that oxygen dopants create local trap states in the band structures of (6,5) SWCNTs. They further studied photon

DOI: 10.1021/acsnano.6b06900
ACS Nano XXXX, XXX, XXX−XXX

antibunching in such oxygen-doped (6,5) SWCNTs and unambiguously demonstrated the observation of single photon emission in such oxygen-doping-induced trapped states in nanotubes. Notably, although the emitted light is still below 1550 nm which is most frequently used in optical communications, it is possible to engineer nanotube-based single photon sources to 1550 nm range, by choosing other chirality nanotubes with smaller band gaps and then using the similar low-concentration oxygen doping method. The wide choices of SWCNTs with different chiralities and therefore different electronic structures offer a feasible way to tune the wavelength of emitted light, which has advantages and is complementary to other solid-state single photon sources such as colored centers in diamond and monolayer WSe_2 materials which emit light in the visible light region.[136,137]

OPPORTUNITIES AND OUTLOOK

Growth Innovations. It is clear that substantial progresses have been made by scientists worldwide toward chirality-controlled growth of SWCNTs. Many factors may affect the chirality distribution of as-grown SWCNTs, making chirality control of CNT a formidable task. Noticeably, recent experiments have clearly shown that the catalyst is the most deterministic one among many factors in modulating the chirality of CNTs during the growth process. Many aspects of the properties of catalysts, including their chemical compositions and physical states, sizes, shapes, pretreatment conditions, have been extensively studied, and now the purity of single-chirality SWCNT species have been improved continuously thanks to many researchers' efforts in catalyst engineering. However, controlled growth of pure SWCNTs with specific chirality is still not possible at this stage. More growth innovations such as further development of catalysts and exploration and optimization of the growth process will definitely be necessary to solve the nanotube chirality problem. Here we raise some key questions and offer our perspectives toward chirality-controlled growth of SWCNTs in the spirit of stimulating further explorations in this important direction.

(1) How can one prepare crystalline NP catalysts with excellent high-temperature stability and identical composition and size? The use of metal NP-based catalysts for chirality-enriched growth of SWCNTs has been reported extensively, and great success has been made recently. The chirality selectivity is believed to stem from the epitaxial relationship between solid crystalline NP catalysts and specific chiralities of CNTs. However, currently one cannot prepare small NPs with identical composition, size, shape, *etc*. Moreover, even when we start from NP catalysts with identical properties, how to completely suppress or minimize changes of these NPs, which can be caused by high-temperature processing or interactions of NP catalysts with underlying substrates and surrounding gaseous environments, is worth critical thinking and further development.

(2) How can one improve the yield of nanotube cloning? The nanotube cloning method, in principle, could grow single-chirality SWCNTs if the seeds used are 100% pure. On one hand, this request calls for further development of postsynthesis separation approaches to improve the purity of single-chirality nanotubes. On the other hand, so far the yield and efficiency of nanotube cloning is quite low, and some key questions such as how carbon species are added to the open-ends of nanotube seeds and how new CNT segments grow are still poorly understood. Comparative studies of nanotube cloning from nanotube seeds with different chiralities or wrapped by different surfactants can shine a light on a better understanding of the cloning process,[16,35] and there needs to be further detailed studies.

(3) How can one maintain the original structures of carbonaceous molecular seeds? One key advantage of molecular seeds compared with NP catalysts and separated nanotube seeds is that these molecules are identical prior to CNT growth. Unfortunately, recent results have shown that these small molecules underwent irreversible structural changes at high growth temperatures.[56,59] Therefore, how to maintain the molecule structure intact during CNT growth process, for example, by lowering the growth temperature significantly, could be a promising way to solve the nanotube chirality problem. SWCNT growth usually requires high temperatures to decompose carbon sources and heal defects of as-grown SWCNTs. One approach is to use certain types of external means such as plasma to assist the decomposition of less thermally stable carbon-containing precursors like C_2H_2. This approach can further be combined with low-temperature SWCNT growth (which may produce defective SWCNTs), followed by a postgrowth high-temperature graphitization (annealing) process to improve the quality of SWCNTs while maintaining their chirality defined by the original molecular seeds.

(4) Development of the nanotube growth process. Nowadays CVD is the most commonly used method to grow CNTs, and most achievements in chirality-controlled synthesis of CNTs were made using CVD methods. We note that most CNT CVD processes are operated in pressure ranges of rough vacuum (10^{-3} Torr) to several atmosphere pressures. In such processes, there exist numerous gaseous species and gas-phase and on-substrate reactions, which make the CNT growth process very complicated. If we can grow CNTs under a more "clean" system, can we achieve better selectivity and controllability? For example, in a high-vacuum molecular beam epitaxy (MBE) process, which is known to have very good process controllability, the structures of newly grown materials can be precisely controlled by the substrates *via* epitaxial relationship. If we do CNT synthesis in a MBE-like fashion, can we eliminate all other unwanted reactions and achieve a good selectivity? Such processes may decrease the yield and increase the cost of CNT growth, but it is still meaningful if one can achieve a better control of CNT chirality. In addition, previous reports have indicated that single-chirality (2,2) CNTs can be formed inside the channels of zeolite template, despite that such ultrasmall CNTs would decompose without confinement of template.[139] These results suggest that design and exploration of suitable templates or substrates that have very strong interactions with certain types of CNTs could also be an interesting approach to try besides catalyst engineering. Furthermore, the charge transfer from catalyst nanoparticles to the growing nanotube edge atoms was studied and found to play a role in enhancing the reactivity of growth edges by changing their frontier electron density, which implies

DOI: 10.1021/acsnano.6b06900
ACS Nano XXXX, XXX, XXX−XXX

that the growth active sites are strongly correlated with the structures of metal nanoparticles through charge transfer.[140] Thus, charge transfer engineering between the growing nanotubes and the catalyst nanoparticles may be a way to tailor the growth selectivity. A more recent publication has shown that SWCNTs are negatively charged during CVD growth, and charged SWCNTs may have influence on the chirality distribution of as-grown samples.[141] This discovery may open up a possibility to control the chirality of as-grown SWCNTs through electrochemical methods, which has drawn very little attention previously.

(5) Growth kinetics *versus* thermodynamics. Experimental results from many groups have clearly shown the enrichment of near-armchair $(n,n-1)$ SWCNTs in very diverse growth processes. This fact indicates that there must be some unique points for these near-armchair SWCNTs. There are two possible attributes that can lead to the enrichment of near-armchair CNTs. The first is thermodynamics, *i.e.*, near-armchair SWCNTs may be more stable and therefore, the number of near-armchair SWCNTs is more than other nanotubes in a sample. The second is kinetics, *i.e.*, near-armchair SWCNTs may grow faster and consequently have longer lengths than other nanotubes. We note that either reason could result in an enrichment of near-armchair SWCNTs[7,19] based on many kinds of characterization including direct imaging and spectroscopy methods. It is also possible that both thermodynamic and kinetic processes may have influence on the final chirality distribution of a SWCNT ensemble. These results also suggest to us to take both reasons into consideration when designing our growth process. There is no doubt that the comparative investigations of nucleation, growth, termination, and reaction behavior on individual nanotube level with known chirality are important to elucidate many aspects of these questions.

(6) Lessons from nanotube separation. Several nanotube separation methods have been well-documented to be able to produce single-chirality SWCNTs with purity higher than 90%, while direct growth of single-chirality SWCNTs with purity higher than 90% is still elusive. One noticeable difference between separation and growth processes is that in nanotube separation, the chiral dispersant molecules (DNA, bile salts, *etc.*) interact with the entire nanotube surface over the length range of a few hundred nanometers to a few micrometers. A small difference among different nanotube species in dispersant/nanotube binding energy per unit length can be amplified into a large one through integration over the entire nanotube length, resulting in high selectivity in separation. As a comparison, in the nanotube growth process, the nanotube/catalyst interfaces, which determine the chirality selectivity of the as-grown nanotubes, cover much shorter length scales, ranging from subnanometer to a few nanometers. The nanotube/catalyst binding energy difference among different nanotube species may be too small to effectively impact the chirality selectivity due to the much shorter interaction length between nanotubes and catalysts. Therefore, a lesson that the nanotube-growth community can learn from the nanotube-separation community is to increase the interaction length between nanotubes and the growth environment, including but not limited to catalysts and growth substrates. While numerous efforts have been devoted to the exploration of new catalysts aiming for chirality-controlled growth of nanotubes, there exist few studies on the design of novel substrates for nanotube controlled-growth. Imagining if there is a special growth substrate which can selectively bind with a specific (n,m) nanotube, in principle, one may be able to achieve the selective growth of this specific chirality nanotube with high purity. To explore this possibility, more efforts should be given to the study of novel substrates such as recently emerged 2D crystals, for the chirality-controlled growth of nanotubes.

The Relationship between Chirality Control and Handedness Control. There is another level of fine structures of SWCNTs beyond chirality, which is called handedness, and handedness control of SWCNTs has very rarely been studied so far from the direct controlled growth approach.[142] From the atomic structure point of view, a left-handed nanotube is structurally distinct from its mirror image right-handed nanotube. Consequently, a full chirality map of SWCNTs should include both right-handed and left-handed domain (Figure 13). In common practice, however, only half of the chirality map is shown because the electronic structures of an enantiomer pair are identical. This simplification in our opinion has some unintended consequences: There has been little research on handedness control at the synthesis level, and not enough thoughts have been given to the observation that there are always an equal amount of left-handed and right-handed tubes present in synthetic mixtures. Recent work by us suggests a need to consider the full chirality map when it comes to structure control. For example, it is found that DNA-based single-chirality purification is almost always accompanied by enantiomer enrichment.[143] This observation leads us to believe that as far as separation is concerned, chirality control and handedness control are two related parts of the same structure control problem. Since left-handed and right-handed CNTs have distinct structures, true structure control implies the ability to distinguish left-handed and right-handed CNTs. We can draw ample support to this notion from biology where structure control is critical: All biomolecules have defined handedness

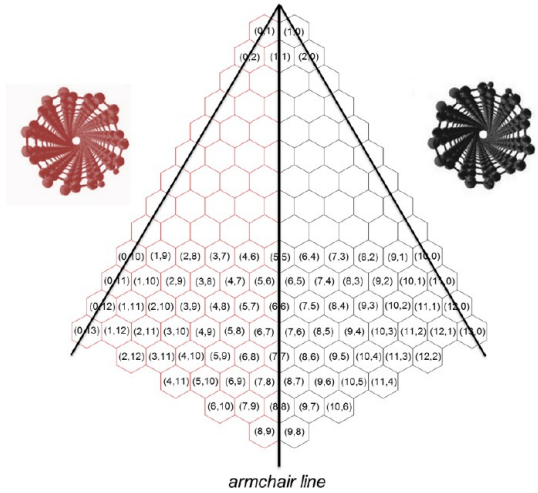

Figure 13. A full chirality map of SWCNTs shows both right- and left-handed species.

DOI: 10.1021/acsnano.6b06900
ACS Nano XXXX, XXX, XXX−XXX

(or homochiral). We propose that a truly structurally controlled synthesis should yield both chirality and enantiomer enrichment, corresponding to one hexagon site on the full chirality map. Using this criterion, we realize that most of the reported structure controlled synthesis is diameter-controlled syntheses along the armchair direction (with few examples showing distribution along zigzag direction),[29,144] with limited control over chirality and no control over handedness. This is probably the result of racemic structures taken by catalyst particles. In this context, the result of Li *et al.* for (12,6) enriched synthesis of SWCNTs is quite remarkable, because the chirality distribution of the synthesized CNTs is off the two special achiral directions (*i.e.*, armchair and zigzag), implying that the catalyst used may have some intrinsic chiral preference. It remains to be seen if the chirality-enriched tubes made by Li *et al.*[14] and many other selective growth methods[7,24,98] are also enantiomer-enriched. Catalyst design in the future should take handedness control into consideration. Likewise, in VPE-based cloning, attention should be paid to the conservation of handedness in addition to chiral indices by the cloned nanotubes.

What Are the Truly Exciting Future Applications of Single-Chirality Carbon Nanotubes? Being able to make structurally well-defined SWCNTs through either separation or synthesis has its intrinsic scientific value. It is also a fair question to ask what the truly exciting and realistic applications of single-chirality tubes are. In the past, many tantalizing CNT-based applications were proposed, ranging from space elevator to armchair quantum wire. While these captured many people's imagination when first proposed some years ago, they still are far away from reality. Now that we know more about CNTs, we should be able to propose something more realistic but still exciting. In the past, a lot of attention has been given to the application of CNTs in electronics, photonics, and optoelectronics. In these cases especially for electronics, the electronic structures of CNTs are certainly important, but the detailed atomic structure of a CNT is not critical: There is no difference between left- and right-handed CNTs and between CNTs of the same diameter but different chiral angles (*e.g.*, (6,5) and (9,1)). Biorelated applications are the place where chirality-defined SWCNTs may find themselves most useful. Biology is enabled by well-defined structures. Biomolecule-nanotube hybrid structures composed of biopolymers of well-defined sequence and SWCNTs of well-defined chirality may be used to construct biomimetic systems, which can facilitate interfacing of electronics with biological system. Another related exciting application is multiplex imaging and sensing through either optical or electronic detections. In this case, SWCNT serves as an optical or electronic reporter whose band gap defines the detection channel, whereas the coating biopolymer confers substrate specificity. Combinatorial diversity of SWCNTs and biopolymer sequences thus provides a huge endowment for these applications. As we have included in this Review, there have been lots of activities in this area already. Further handedness control of nanotubes could provide an additional degree of freedom to play with in these directions.

A True Material for the Future. CNTs are a family of molecules that have many structure varieties and many interesting electronic and optical properties. They are easily interfaced with biomolecules and can be derivatized in a variety of ways by conventional chemistry. We are currently limited by our ability to control their structures, not by the rich endowment of the material itself. If past history tells us anything, it is this: What we cannot do today, we will be able to do tomorrow; what we cannot imagine today, we will be able to realize tomorrow. We encourage young scientists to take on the challenge. The reward will be big.

AUTHOR INFORMATION

Corresponding Authors

*E-mail: chongwuz@usc.edu.
*E-mail: ming.zheng@nist.gov.

ORCID

Bilu Liu: 0000-0002-7274-5752
Ming Zheng: 0000-0002-8058-1348
Chongwu Zhou: 0000-0001-8448-8450

Author Contributions

#These authors contributed equally.

Notes

The authors declare no competing financial interest.

ACKNOWLEDGMENTS

This work was supported by the Air Force Office of Scientific Research (AFOSR). B.L. acknowledges support from the 1000-Talent Program of China, Tsinghua-Berkeley Shenzhen Institute (TBSI), and the Development and Reform Commission of Shenzhen Municipality.

VOCABULARY

Single-wall carbon nanotube, a single-wall carbon nanotube can be conceptually viewed as a seamless rolled-up cylinder from a graphene sheet; **Chirality**, a term used to describe atomic configurations of carbon nanotubes; **Handedness**, a term used to describe enantiomers of carbon nanotubes where a left-handed nanotube is structurally distinct from its mirror image right-handed nanotube; **Chemical vapor deposition**, a commonly used material synthesis technique to deposit solid materials by chemical reaction of gaseous precursors; **Vapor-phase epitaxy**, a widely used epitaxial growth technique to grow high-quality, crystalline semiconducting materials on crystalline substrates using gaseous precursors

REFERENCES

(1) Iijima, S. Helical Microtubules of Graphitic Carbon. *Nature* **1991**, *354*, 56−58.
(2) Iijima, S.; Ichihashi, T. Single-Shell Carbon Nanotubes of 1-Nm Diameter. *Nature* **1993**, *363*, 603−605.
(3) Bethune, D. S.; Kiang, C. H.; Devries, M. S.; Gorman, G.; Savoy, R.; Vazquez, J.; Beyers, R. Cobalt-Catalyzed Growth of Carbon Nanotubes with Single-Atomic-Layerwalls. *Nature* **1993**, *363*, 605−607.
(4) Dai, H. J.; Rinzler, A. G.; Nikolaev, P.; Thess, A.; Colbert, D. T.; Smalley, R. E. Single-Wall Nanotubes Produced by Metal-Catalyzed Disproportionation of Carbon Monoxide. *Chem. Phys. Lett.* **1996**, *260*, 471−475.
(5) Dresselhaus, M. S.; Dresselhaus, G.; Eklund, P. C. *Science of Fullerenes and Carbon Nanotubes: Their Properties and Applications*; Academic Press, Inc.: New York, 1996.
(6) Bronikowski, M. J.; Willis, P. A.; Colbert, D. T.; Smith, K. A.; Smalley, R. E. Gas-Phase Production of Carbon Single-Walled Nanotubes from Carbon Monoxide *via* the HiPco Process: A Parametric Study. *J. Vac. Sci. Technol., A* **2001**, *19*, 1800−1805.
(7) Bachilo, S. M.; Balzano, L.; Herrera, J. E.; Pompeo, F.; Resasco, D. E.; Weisman, R. B. Narrow (n,m)-Distribution of Single-Walled Carbon Nanotubes Grown Using a Solid Supported Catalyst. *J. Am. Chem. Soc.* **2003**, *125*, 11186−11187.

DOI: 10.1021/acsnano.6b06900
ACS Nano XXXX, XXX, XXX−XXX

(8) Wang, Y.; Wei, F.; Luo, G. H.; Yu, H.; Gu, G. S. The Large-Scale Production of Carbon Nanotubes in a Nano-Agglomerate Fluidized-Bed Reactor. *Chem. Phys. Lett.* **2002**, *364*, 568−572.
(9) Cheng, H. M.; Li, F.; Su, G.; Pan, H. Y.; He, L. L.; Sun, X.; Dresselhaus, M. S. Large-Scale and Low-Cost Synthesis of Single-Walled Carbon Nanotubes by the Catalytic Pyrolysis of Hydrocarbons. *Appl. Phys. Lett.* **1998**, *72*, 3282−3284.
(10) Fan, S. S.; Chapline, M. G.; Franklin, N. R.; Tombler, T. W.; Cassell, A. M.; Dai, H. J. Self-Oriented Regular Arrays of Carbon Nanotubes and Their Field Emission Properties. *Science* **1999**, *283*, 512−514.
(11) Ma, W. J.; Song, L.; Yang, R.; Zhang, T. H.; Zhao, Y. C.; Sun, L. F.; Ren, Y.; Liu, D. F.; Liu, L. F.; Shen, J.; Zhang, Z. X.; Xiang, Y. J.; Zhou, W. Y.; Xie, S. S. Directly Synthesized Strong, Highly Conducting, Transparent Single-Walled Carbon Nanotube Films. *Nano Lett.* **2007**, *7*, 2307−2311.
(12) De Volder, M. F. L.; Tawfick, S. H.; Baughman, R. H.; Hart, A. J. Carbon Nanotubes: Present and Future Commercial Applications. *Science* **2013**, *339*, 535−539.
(13) Liu, J.; Wang, C.; Tu, X. M.; Liu, B. L.; Chen, L.; Zheng, M.; Zhou, C. W. Chirality-Controlled Synthesis of Single-Wall Carbon Nanotubes Using Vapour-Phase Epitaxy. *Nat. Commun.* **2012**, *3*, 1199.
(14) Yang, F.; Wang, X.; Zhang, D. Q.; Yang, J.; Luo, D.; Xu, Z. W.; Wei, J. K.; Wang, J. Q.; Xu, Z.; Peng, F.; Li, X. M.; Li, R. M.; Li, Y. L.; Li, M. H.; Bai, X. D.; Ding, F.; Li, Y. Chirality-Specific Growth of Single-Walled Carbon Nanotubes on Solid Alloy Catalysts. *Nature* **2014**, *510*, 522−524.
(15) Sanchez-Valencia, J. R.; Dienel, T.; Groning, O.; Shorubalko, I.; Mueller, A.; Jansen, M.; Amsharov, K.; Ruffieux, P.; Fasel, R. Controlled Synthesis of Single-Chirality Carbon Nanotubes. *Nature* **2014**, *512*, 61−64.
(16) Liu, B. L.; Liu, J.; Tu, X. M.; Zhang, J. L.; Zheng, M.; Zhou, C. W. Chirality-Dependent Vapor-Phase Epitaxial Growth and Termination of Single-Wall Carbon Nanotubes. *Nano Lett.* **2013**, *13*, 4416−4421.
(17) Arenal, R.; Lothman, P.; Picher, M.; Than, T.; Paillet, M.; Jourdain, V. Direct Evidence of Atomic Structure Conservation Along Ultra-Long Carbon Nanotubes. *J. Phys. Chem. C* **2012**, *116*, 14103−14107.
(18) Chiang, W. H.; Sankaran, R. M. Linking Catalyst Composition to Chirality Distributions of As-Grown Single-Walled Carbon Nanotubes by Tuning Ni_xFe_{1-x} Nanoparticles. *Nat. Mater.* **2009**, *8*, 882−886.
(19) Wang, H.; Wei, L.; Ren, F.; Wang, Q.; Pfefferle, L. D.; Haller, G. L.; Chen, Y. Chiral-Selective $CoSO_4/SiO_2$ Catalyst for (9,8) Single-Walled Carbon Nanotube Growth. *ACS Nano* **2013**, *7*, 614−626.
(20) Lolli, G.; Zhang, L. A.; Balzano, L.; Sakulchaicharoen, N.; Tan, Y. Q.; Resasco, D. E. Tailoring (n,m) Structure of Single-Walled Carbon Nanotubes by Modifying Reaction Conditions and the Nature of the Support of CoMo Catalysts. *J. Phys. Chem. B* **2006**, *110*, 2108−2115.
(21) Che, Y. C.; Wang, C.; Liu, J.; Liu, B. L.; Lin, X.; Parker, J.; Beasley, C.; Wong, H. S. P.; Zhou, C. W. Selective Synthesis and Device Applications of Semiconducting Single-Walled Carbon Nanotubes Using Isopropyl Alcohol as Feedstock. *ACS Nano* **2012**, *6*, 7454−7462.
(22) Fouquet, M.; Bayer, B. C.; Esconjauregui, S.; Blume, R.; Warner, J. H.; Hofmann, S.; Schlogl, R.; Thomsen, C.; Robertson, J. Highly Chiral-Selective Growth of Single-Walled Carbon Nanotubes with a Simple Monometallic Co Catalyst. *Phys. Rev. B: Condens. Matter Mater. Phys.* **2012**, *85*, 235411.
(23) He, M.; Chernov, A. I.; Fedotov, P. V.; Obraztsova, E. D.; Sainio, J.; Rikkinen, E.; Jiang, H.; Zhu, Z.; Tian, Y.; Kauppinen, E. I.; Niemela, M.; Krauset, A. O. I. Predominant (6,5) Single-Walled Carbon Nanotube Growth on a Copper-Promoted Iron Catalyst. *J. Am. Chem. Soc.* **2010**, *132*, 13994−13996.
(24) Liu, B. L.; Ren, W. C.; Li, S. S.; Liu, C.; Cheng, H. M. High Temperature Selective Growth of Single-Walled Carbon Nanotubes with a Narrow Chirality Distribution from a CoPt Bimetallic Catalyst. *Chem. Commun.* **2012**, *48*, 2409−2411.
(25) Li, X. L.; Tu, X. M.; Zaric, S.; Welsher, K.; Seo, W. S.; Zhao, W.; Dai, H. J. Selective Synthesis Combined with Chemical Separation of Single-Walled Carbon Nanotubes for Chirality Selection. *J. Am. Chem. Soc.* **2007**, *129*, 15770−15771.
(26) Zhao, Q. C.; Xu, Z. W.; Hu, Y.; Ding, F.; Zhang, J. Chemical Vapor Deposition Synthesis of Near-Zigzag Single-Walled Carbon Nanotubes with Stable Tube-Catalyst Interface. *Sci. Adv.* **2016**, *2*, e1501729.
(27) Zhu, Z.; Jiang, H.; Susi, T.; Nasibulin, A. G.; Kauppinen, E. I. The Use of NH_3 to Promote the Production of Large-Diameter Single-Walled Carbon Nanotubes with a Narrow (n,m) Distribution. *J. Am. Chem. Soc.* **2011**, *133*, 1224−1227.
(28) Harutyunyan, A. R.; Chen, G. G.; Paronyan, T. M.; Pigos, E. M.; Kuznetsov, O. A.; Hewaparakrama, K.; Kim, S. M.; Zakharov, D.; Stach, E. A.; Sumanasekera, G. U. Preferential Growth of Single-Walled Carbon Nanotubes with Metallic Conductivity. *Science* **2009**, *326*, 116−120.
(29) Yang, F.; Wang, X.; Zhang, D.; Qi, K.; Yang, J.; Xu, Z.; Li, M.; Zhao, X.; Bai, X.; Li, Y. Growing Zigzag (16,0) Carbon Nanotubes with Structure-Defined Catalysts. *J. Am. Chem. Soc.* **2015**, *137*, 8688−8691.
(30) Tu, X. M.; Manohar, S.; Jagota, A.; Zheng, M. DNA Sequence Motifs for Structure-Specific Recognition and Separation of Carbon Nanotubes. *Nature* **2009**, *460*, 250−253.
(31) Tu, X. M.; Walker, A. R. H.; Khripin, C. Y.; Zheng, M. Evolution of DNA Sequences Toward Recognition of Metallic Armchair Carbon Nanotubes. *J. Am. Chem. Soc.* **2011**, *133*, 12998−13001.
(32) Smalley, R. E.; Li, Y. B.; Moore, V. C.; Price, B. K.; Colorado, R.; Schmidt, H. K.; Hauge, R. H.; Barron, A. R.; Tour, J. M. Single Wall Carbon Nanotube Amplification: En Route to a Type-Specific Growth Mechanism. *J. Am. Chem. Soc.* **2006**, *128*, 15824−15829.
(33) Wang, Y. H.; Kim, M. J.; Shan, H. W.; Kittrell, C.; Fan, H.; Ericson, L. M.; Hwang, W. F.; Arepalli, S.; Hauge, R. H.; Smalley, R. E. Continued Growth of Single-Walled Carbon Nanotubes. *Nano Lett.* **2005**, *5*, 997−1002.
(34) Yao, Y. G.; Feng, C. Q.; Zhang, J.; Liu, Z. F. "Cloning" of Single-Walled Carbon Nanotubes *via* Open-End Growth Mechanism. *Nano Lett.* **2009**, *9*, 1673−1677.
(35) Wang, H.; Yamada, C.; Liu, J.; Liu, B. L.; Tu, X. M.; Zheng, M.; Zhou, C. W.; Homma, Y. Re-Growth of Single-Walled Carbon Nanotube by Hot-Wall and Cold-Wall Chemical Vapor Deposition. *Carbon* **2015**, *95*, 497−502.
(36) Hong, G.; Chen, Y. B.; Li, P.; Zhang, J. Controlling the Growth of Single-Walled Carbon Nanotubes on Surfaces Using Metal and Non-Metal Catalysts. *Carbon* **2012**, *50*, 2067−2082.
(37) Takagi, D.; Homma, Y.; Hibino, H.; Suzuki, S.; Kobayashi, Y. Single-Walled Carbon Nanotube Growth from Highly Activated Metal Nanoparticles. *Nano Lett.* **2006**, *6*, 2642−2645.
(38) Yuan, D. N.; Ding, L.; Chu, H. B.; Feng, Y. Y.; McNicholas, T. P.; Liu, J. Horizontally Aligned Single-Walled Carbon Nanotube on Quartz from a Large Variety of Metal Catalysts. *Nano Lett.* **2008**, *8*, 2576−2579.
(39) Liu, B. L.; Ren, W. C.; Gao, L. B.; Li, S. S.; Liu, Q. F.; Jiang, C. B.; Cheng, H. M. Manganese-Catalyzed Surface Growth of Single-Walled Carbon Nanotubes with High Efficiency. *J. Phys. Chem. C* **2008**, *112*, 19231−19235.
(40) Zhou, W. W.; Han, Z. Y.; Wang, J. Y.; Zhang, Y.; Jin, Z.; Sun, X.; Zhang, Y. W.; Yan, C. H.; Li, Y. Copper Catalyzing Growth of Single-Walled Carbon Nanotubes on Substrates. *Nano Lett.* **2006**, *6*, 2987−2990.
(41) Bhaviripudi, S.; Mile, E.; Steiner, S. A.; Zare, A. T.; Dresselhaus, M. S.; Belcher, A. M.; Kong, J. CVD Synthesis of Single-Walled Carbon Nanotubes from Gold Nanoparticle Catalysts. *J. Am. Chem. Soc.* **2007**, *129*, 1516−1517.
(42) He, M. S.; Jiang, H.; Liu, B. L.; Fedotov, P. V.; Chernov, A. I.; Obraztsova, E. D.; Cavalca, F.; Wagner, J. B.; Hansen, T. W.; Anoshkin, I. V.; Obraztsova, E. A.; Belkin, A. V.; Sairanen, E.;

DOI: 10.1021/acsnano.6b06900
ACS Nano XXXX, XXX, XXX−XXX

Nasibulin, A. G.; Lehtonen, J.; Kauppinen, E. I. Chiral-Selective Growth of Single-Walled Carbon Nanotubes on Lattice-Mismatched Epitaxial Cobalt Nanoparticles. *Sci. Rep.* **2013**, *3*, 1460.
(43) Wang, H.; Wang, B.; Quek, X. Y.; Wei, L.; Zhao, J. W.; Li, L. J.; Chan-Park, M. B.; Yang, Y. H.; Chen, Y. Selective Synthesis of (9,8) Single Walled Carbon Nanotubes on Cobalt Incorporated TUD-1 Catalysts. *J. Am. Chem. Soc.* **2010**, *132*, 16747−16749.
(44) Yuan, Y.; Karahan, H. E.; Yildirim, C.; Wei, L.; Birer, O.; Zhai, S. L.; Lau, R.; Chen, Y. "Smart Poisoning" of Co/SiO_2 Catalysts by Sulfidation for Chirality-Selective Synthesis of (9,8) Single-Walled Carbon Nanotubes. *Nanoscale* **2016**, *8*, 17705−17713.
(45) Zhu, H. W.; Suenaga, K.; Wei, J. Q.; Wang, K. L.; Wu, D. H. A Strategy to Control the Chirality of Single-Walled Carbon Nanotubes. *J. Cryst. Growth* **2008**, *310*, 5473−5476.
(46) Liu, B. L.; Ren, W. C.; Gao, L. B.; Li, S. S.; Pei, S. F.; Liu, C.; Jiang, C. B.; Cheng, H. M. Metal-Catalyst-Free Growth of Single-Walled Carbon Nanotubes. *J. Am. Chem. Soc.* **2009**, *131*, 2082−2083.
(47) Liu, B. L.; Ren, W. C.; Liu, C.; Sun, C. H.; Gao, L. B.; Li, S. S.; Jiang, C. B.; Cheng, H. M. Growth Velocity and Direct Length-Sorted Growth of Short Single-Walled Carbon Nanotubes by a Metal-Catalyst-Free Chemical Vapor Deposition Process. *ACS Nano* **2009**, *3*, 3421−3430.
(48) Liu, B. L.; Tang, D. M.; Sun, C. H.; Liu, C.; Ren, W. C.; Li, F.; Yu, W. J.; Yin, L. C.; Zhang, L. L.; Jiang, C. B.; Cheng, H. M. Importance of Oxygen in the Metal-Free Catalytic Growth of Single-Walled Carbon Nanotubes from SiO_x by a Vapor-Solid-Solid Mechanism. *J. Am. Chem. Soc.* **2011**, *133*, 197−199.
(49) Huang, S. M.; Cai, Q. R.; Chen, J. Y.; Qian, Y.; Zhang, L. J. Metal-Catalyst-Free Growth of Single-Walled Carbon Nanotubes on Substrates. *J. Am. Chem. Soc.* **2009**, *131*, 2094−2095.
(50) Takagi, D.; Hibino, H.; Suzuki, S.; Kobayashi, Y.; Homma, Y. Carbon Nanotube Growth from Semiconductor Nanoparticles. *Nano Lett.* **2007**, *7*, 2272−2275.
(51) Yang, F.; Wang, X.; Si, J.; Zhao, X.; Qi, K.; Jin, C.; Zhang, Z.; Li, M.; Zhang, D.; Yang, J.; Zhang, Z.; Xu, Z.; Peng, L. M.; Bai, X.; Li, Y. Water-Assisted Preparation of High-Purity Semiconducting (14,4) Carbon Nanotubes. *ACS Nano* **2016**, DOI: 10.1021/acsnano.6b06890.
(52) Liu, B.; Jiang, H.; Krasheninnikov, A. V.; Nasibulin, A. G.; Ren, W.; Liu, C.; Kauppinen, E. I.; Cheng, H. M. Chirality-Dependent Reactivity of Individual Single-Walled Carbon Nanotubes. *Small* **2013**, *9*, 1379−1386.
(53) Mueller, A.; Amsharov, K. Y.; Jansen, M. End-Cap Precursor Molecules for the Controlled Growth of Single-Walled Carbon Nanotubes. *Fullerenes, Nanotubes, Carbon Nanostruct.* **2012**, *20*, 401−404.
(54) Scott, L. T.; Jackson, E. A.; Zhang, Q. Y.; Steinberg, B. D.; Bancu, M.; Li, B. A Short, Rigid, Structurally Pure Carbon Nanotube by Stepwise Chemical Synthesis. *J. Am. Chem. Soc.* **2012**, *134*, 107−110.
(55) Omachi, H.; Segawa, Y.; Itami, K. Synthesis of Cycloparaphenylenes and Related Carbon Nanorings: A Step toward the Controlled Synthesis of Carbon Nanotubes. *Acc. Chem. Res.* **2012**, *45*, 1378−1389.
(56) Omachi, H.; Nakayama, T.; Takahashi, E.; Segawa, Y.; Itami, K. Initiation of Carbon Nanotube Growth by Well-Defined Carbon Nanorings. *Nat. Chem.* **2013**, *5*, 572−576.
(57) Rao, F.; Li, T.; Wang, Y. L. Growth of "All-Carbon" Single-Walled Carbon Nanotubes from Diamonds and Fullerenes. *Carbon* **2009**, *47*, 3580−3584.
(58) Yu, X. C.; Zhang, J.; Choi, W.; Choi, J. Y.; Kim, J. M.; Gan, L. B.; Liu, Z. F. Cap Formation Engineering: From Opened C_{60} to Single-Walled Carbon Nanotubes. *Nano Lett.* **2010**, *10*, 3343−3349.
(59) Liu, B. L.; Liu, J.; Li, H. B.; Bhola, R.; Jackson, E. A.; Scott, L. T.; Page, A.; Irle, S.; Morokuma, K.; Zhou, C. W. Nearly Exclusive Growth of Small Diameter Semiconducting Single-Wall Carbon Nanotubes from Organic Chemistry Synthetic End-Cap Molecules. *Nano Lett.* **2015**, *15*, 586−595.
(60) Haroz, E.; Duque, J. G.; Barros, E. B.; Telg, H.; Simpson, J. R.; Walker, A. R. H.; Khripin, C. Y.; Fagan, J. A.; Tu, X.; Zheng, M.; Kono, J.; Doorn, S. K. Asymmetric Excitation Profiles in the Resonance Raman Response of Armchair Carbon Nanotubes. *Phys. Rev. B: Condens. Matter Mater. Phys.* **2015**, *91*, 205446.
(61) Ding, F.; Harutyunyan, A. R.; Yakobson, B. I. Dislocation Theory of Chirality-Controlled Nanotube Growth. *Proc. Natl. Acad. Sci. U. S. A.* **2009**, *106*, 2506−2509.
(62) Li, H. B.; Page, A. J.; Irle, S.; Morokuma, K. Single-Walled Carbon Nanotube Growth from Chiral Carbon Nanorings: Prediction of Chirality and Diameter Influence on Growth Rates. *J. Am. Chem. Soc.* **2012**, *134*, 15887−15896.
(63) Wang, Q.; Ng, M. F.; Yang, S. W.; Yang, Y. H.; Chen, Y. A. The Mechanism of Single-Walled Carbon Nanotube Growth and Chirality Selection Induced by Carbon Atom and Dimer Addition. *ACS Nano* **2010**, *4*, 939−946.
(64) Artyukhov, V. I.; Penev, E. S.; Yakobson, B. I. Why Nanotubes Grow Chiral. *Nat. Commun.* **2014**, *5*, 4892.
(65) Yuan, Q.; Ding, F. How a Zigzag Carbon Nanotube Grows. *Angew. Chem.* **2015**, *127*, 6022−6026.
(66) Hirahara, K.; Kociak, M.; Bandow, S.; Nakahira, T.; Itoh, K.; Saito, Y.; Iijima, S. Chirality Correlation in Double-Wall Carbon Nanotubes as Studied by Electron Diffraction. *Phys. Rev. B: Condens. Matter Mater. Phys.* **2006**, *73*, 195420.
(67) Rao, R.; Liptak, D.; Cherukuri, T.; Yakobson, B. I.; Maruyama, B. *In Situ* Evidence for Chirality-Dependent Growth Rates of Individual Carbon Nanotubes. *Nat. Mater.* **2012**, *11*, 213−216.
(68) Dumlich, H.; Reich, S. Chirality-Dependent Growth Rate of Carbon Nanotubes: A Theoretical Study. *Phys. Rev. B: Condens. Matter Mater. Phys.* **2010**, *82*, 085421.
(69) Liu, B.; Wang, C.; Liu, J.; Che, Y.; Zhou, C. Aligned Carbon Nanotubes: from Controlled Synthesis to Electronic Applications. *Nanoscale* **2013**, *5*, 9483−9502.
(70) Yu, B.; Hou, P. X.; Li, F.; Liu, B. L.; Liu, C.; Cheng, H. M. Selective Removal of Metallic Single-Walled Carbon Nanotubes by Combined *in Situ* and Post-Synthesis Oxidation. *Carbon* **2010**, *48*, 2941−2947.
(71) Yu, B.; Liu, C.; Hou, P. X.; Tian, Y.; Li, S. S.; Liu, B. L.; Li, F.; Kauppinen, E. I.; Cheng, H. M. Bulk Synthesis of Large Diameter Semiconducting Single-Walled Carbon Nanotubes by Oxygen-Assisted Floating Catalyst Chemical Vapor Deposition. *J. Am. Chem. Soc.* **2011**, *133*, 5232−5235.
(72) Zhou, W. W.; Zhan, S. T.; Ding, L.; Liu, J. General Rules for Selective Growth of Enriched Semiconducting Single Walled Carbon Nanotubes with Water Vapor as *in Situ* Etchant. *J. Am. Chem. Soc.* **2012**, *134*, 14019−14026.
(73) Li, J. H.; Ke, C. T.; Liu, K. H.; Li, P.; Liang, S. H.; Finkelstein, G.; Wang, F.; Liu, J. Importance of Diameter Control on Selective Synthesis of Semiconducting Single-Walled Carbon Nanotubes. *ACS Nano* **2014**, *8*, 8564−8572.
(74) Qin, X. J.; Peng, F.; Yang, F.; He, X. H.; Huang, H. X.; Luo, D.; Yang, J.; Wang, S.; Liu, H. C.; Peng, L. M.; Li, Y. Growth of Semiconducting Single-Walled Carbon Nanotubes by Using Ceria as Catalyst Supports. *Nano Lett.* **2014**, *14*, 512−517.
(75) Ding, L.; Tselev, A.; Wang, J. Y.; Yuan, D. N.; Chu, H. B.; McNicholas, T. P.; Li, Y.; Liu, J. Selective Growth of Well-Aligned Semiconducting Single-Walled Carbon Nanotubes. *Nano Lett.* **2009**, *9*, 800−805.
(76) Kang, L. X.; Hu, Y.; Liu, L. L.; Wu, J. X.; Zhang, S. C.; Zhao, Q. C.; Ding, F.; Li, Q. W.; Zhang, J. Growth of Close-Packed Semiconducting Single-Walled Carbon Nanotube Arrays Using Oxygen-Deficient TiO_2 Nanoparticles as Catalysts. *Nano Lett.* **2015**, *15*, 403−409.
(77) Zhang, F.; Hou, P. X.; Liu, C.; Wang, B. W.; Jiang, H.; Chen, M. L.; Sun, D. M.; Li, J. C.; Cong, H. T.; Kauppinen, E. I.; Cheng, H. M. Growth of Semiconducting Single-Wall Carbon Nanotubes with a Narrow Band-Gap Distribution. *Nat. Commun.* **2016**, *7*, 11160.
(78) Zheng, M.; Diner, B. A. Solution Redox Chemistry of Carbon Nanotubes. *J. Am. Chem. Soc.* **2004**, *126*, 15490−15494.
(79) Zheng, M.; Semke, E. D. Enrichment of Single Chirality Carbon Nanotubes. *J. Am. Chem. Soc.* **2007**, *129*, 6084−6085.

DOI: 10.1021/acsnano.6b06900
ACS Nano XXXX, XXX, XXX−XXX

(80) Arnold, M. S.; Green, A. A.; Hulvat, J. F.; Stupp, S. I.; Hersam, M. C. Sorting Carbon Nanotubes by Electronic Structure Using Density Differentiation. *Nat. Nanotechnol.* **2006**, *1*, 60−65.
(81) Green, A. A.; Hersam, M. C. Nearly Single-Chirality Single-Walled Carbon Nanotubes Produced *via* Orthogonal Iterative Density Gradient Ultracentrifugation. *Adv. Mater.* **2011**, *23*, 2185−2190.
(82) Ha, M. J.; Xia, Y.; Green, A. A.; Zhang, W.; Renn, M. J.; Kim, C. H.; Hersam, M. C.; Frisbie, C. D. Printed, Sub-3V Digital Circuits on Plastic from Aqueous Carbon Nanotube Inks. *ACS Nano* **2010**, *4*, 4388−4395.
(83) Ghosh, S.; Bachilo, S. M.; Weisman, R. B. Advanced Sorting of Single-Walled Carbon Nanotubes by Nonlinear Density-Gradient Ultracentrifugation. *Nat. Nanotechnol.* **2010**, *5*, 443−450.
(84) Liu, H.; Nishide, D.; Tanaka, T.; Kataura, H. Large-Scale Single-Chirality Separation of Single-Wall Carbon Nanotubes by Simple Gel Chromatography. *Nat. Commun.* **2011**, *2*, 309.
(85) Gui, H.; Li, H.; Tan, F.; Jin, H.; Zhang, J.; Li, Q. Binary Gradient Elution of Semiconducting Single-Walled Carbon Nanotubes by Gel Chromatography for Their Separation According to Chirality. *Carbon* **2012**, *50*, 332−335.
(86) Liu, H. P.; Tanaka, T.; Urabe, Y.; Kataura, H. High-Efficiency Single-Chirality Separation of Carbon Nanotubes Using Temperature-Controlled Gel Chromatography. *Nano Lett.* **2013**, *13*, 1996−2003.
(87) Tanaka, T.; Urabe, Y.; Hirakawa, T.; Kataura, H. Simultaneous Chirality and Enantiomer Separation of Metallic Single-Wall Carbon Nanotubes by Gel Column Chromatography. *Anal. Chem.* **2015**, *87*, 9467−9472.
(88) Yomogida, Y.; Tanaka, T.; Zhang, M. F.; Yudasaka, M.; Wei, X. J.; Kataura, H. Industrial-Scale Separation of High-Purity Single-Chirality Single-Wall Carbon Nanotubes for Biological Imaging. *Nat. Commun.* **2016**, *7*, 12056.
(89) Khripin, C. Y.; Fagan, J. A.; Zheng, M. Spontaneous Partition of Carbon Nanotubes in Polymer-Modified Aqueous Phases. *J. Am. Chem. Soc.* **2013**, *135*, 6822−6825.
(90) Zaslavsky, B. Y. Aqueous Two-Phase Partitioning. In *Physical Chemistry and Bioanalytical Applications*; Marcel Dekker: New York, 1995; pp 694.
(91) Albertsson, P.-A. *Partition of Cell Particles and Macromoleucles*, 2nd ed.; John Wiley and Sons: Chichester, 1971.
(92) Zhang, M.; Khripin, C. Y.; Fagan, J. A.; McPhie, P.; Ito, Y.; Zheng, M. Single-Step Total Fractionation of Single-Wall Carbon Nanotubes by Countercurrent Chromatography. *Anal. Chem.* **2014**, *86*, 3980−3984.
(93) Fagan, J. A.; Khripin, C. Y.; Silvera Batista, C. A.; Simpson, J. R.; Haroz, E. H.; Hight Walker, A. R.; Zheng, M. Isolation of Specific Small-Diameter Single-Wall Carbon Nanotube Species *via* Aqueous Two-Phase Extraction. *Adv. Mater.* **2014**, *26*, 2800−2804.
(94) Fagan, J. A.; Haroz, E. H.; Ihly, R.; Gui, H.; Blackburn, J. L.; Simpson, J. R.; Lam, S.; Hight Walker, A. R.; Doorn, S. K.; Zheng, M. Isolation of > 1 nm Diameter Single-Wall Carbon Nanotube Species Using Aqueous Two-Phase Extraction. *ACS Nano* **2015**, *9*, 5377−5390.
(95) Ao, G.; Khripin, C. Y.; Zheng, M. DNA-Controlled Partition of Carbon Nanotubes in Polymer Aqueous Two-Phase Systems. *J. Am. Chem. Soc.* **2014**, *136*, 10383−10392.
(96) Fagan, J. A.; Haroz, E. H.; Ihly, R.; Gui, H.; Blackburn, J. L.; Simpson, J. R.; Lam, S.; Walker, A. R. H.; Doorn, S. K.; Zheng, M. Isolation of > 1 nm Diameter Single-Wall Carbon Nanotube Species Using Aqueous Two-Phase Extraction. *ACS Nano* **2015**, *9*, 5377−5390.
(97) Zhao, Q.; Zhang, J. Characterizing the Chiral Index of a Single-Walled Carbon Nanotube. *Small* **2014**, *10*, 4586−4605.
(98) Maruyama, S.; Kojima, R.; Miyauchi, Y.; Chiashi, S.; Kohno, M. Low-Temperature Synthesis of High-Purity Single-Walled Carbon Nanotubes from Alcohol. *Chem. Phys. Lett.* **2002**, *360*, 229−234.
(99) Jiang, H.; Nasibulin, A. G.; Brown, D. P.; Kauppinen, E. I. Unambiguous Atomic Structural Determination of Single-Walled Carbon Nanotubes by Electron Diffraction. *Carbon* **2007**, *45*, 662−667.
(100) Liu, K. H.; Wang, W. L.; Xu, Z.; Bai, X. D.; Wang, E. G.; Yao, Y. G.; Zhang, J.; Liu, Z. F. Chirality-Dependent Transport Properties of Double-Walled Nanotubes Measured *in Situ* on Their Field-Effect Transistors. *J. Am. Chem. Soc.* **2009**, *131*, 62−63.
(101) Liu, K. H.; Deslippe, J.; Xiao, F. J.; Capaz, R. B.; Hong, X. P.; Aloni, S.; Zettl, A.; Wang, W. L.; Bai, X. D.; Louie, S. G.; Wang, E. G.; Wang, F. An Atlas of Carbon Nanotube Optical Transitions. *Nat. Nanotechnol.* **2012**, *7*, 325−329.
(102) Liu, K. H.; Hong, X. P.; Choi, S.; Jin, C. H.; Capaz, R. B.; Kim, J.; Wang, W. L.; Bai, X. D.; Louie, S. G.; Wang, E. G.; Wang, F. Systematic Determination of Absolute Absorption Cross-Section of Individual Carbon Nanotubes. *Proc. Natl. Acad. Sci. U. S. A.* **2014**, *111*, 7564−7569.
(103) Liu, K. H.; Hong, X. P.; Zhou, Q.; Jin, C. H.; Li, J. H.; Zhou, W. W.; Liu, J.; Wang, E. G.; Zettl, A.; Wang, F. High-Throughput Optical Imaging and Spectroscopy of Individual Carbon Nanotubes in Devices. *Nat. Nanotechnol.* **2013**, *8*, 917−922.
(104) He, M. S.; Liu, B. L.; Chernov, A. I.; Obraztsova, E. D.; Kauppi, I.; Jiang, H.; Anoshkin, I.; Cavalca, F.; Hansen, T. W.; Wagner, J. B.; Nasibulin, A. G.; Kauppinen, E. I.; Linnekoski, J.; Niemela, M.; Lehtonen, J. Growth Mechanism of Single-Walled Carbon Nanotubes on Iron-Copper Catalyst and Chirality Studies by Electron Diffraction. *Chem. Mater.* **2012**, *24*, 1796−1801.
(105) Lee, H. W.; Yoon, Y.; Park, S.; Oh, J. H.; Hong, S.; Liyanage, L. S.; Wang, H. L.; Morishita, S.; Patil, N.; Park, Y. J.; Park, J. J.; Spakowitz, A.; Galli, G.; Gygi, F.; Wong, P. H. S.; Tok, J. B. H.; Kim, J. M.; Bao, Z. A. Selective Dispersion of High Purity Semiconducting Single-Walled Carbon Nanotubes with Regioregular Poly(3-Alkylthiophene)s. *Nat. Commun.* **2011**, *2*, 541.
(106) Wu, W.; Yue, J.; Lin, X.; Li, D.; Zhu, F.; Yin, X.; Zhu, J.; Wang, J.; Zhang, J.; Chen, Y.; Wang, X.; Li, T.; He, Y.; Dai, X.; Liu, P.; Wei, Y.; Wang, J.; Zhang, W.; Huang, Y.; Fan, L.; Zhang, L.; Li, Q.; Fan, S.; Jiang, K. True-Color Real-Time Imaging and Spectroscopy of Carbon Nanotubes on Substrates Using Enhanced Rayleigh Scattering. *Nano Res.* **2015**, *8*, 2721−2732.
(107) Wu, W.; Yue, J.; Li, D.; Lin, X.; Zhu, F.; Yin, X.; Zhu, J.; Dai, X.; Liu, P.; Wei, Y.; Wang, J.; Yang, H.; Zhang, L.; Li, Q.; Fan, S.; Jiang, K. Interface Dipole Enhancement Effect and Enhanced Rayleigh Scattering. *Nano Res.* **2015**, *8*, 303−319.
(108) Du, J. H.; Pei, S. F.; Ma, L. P.; Cheng, H. M. 25th Anniversary Article: Carbon Nanotube- and Graphene- Based Transparent Conductive Films for Optoelectronic Devices. *Adv. Mater.* **2014**, *26*, 1958−1991.
(109) Wei, L.; Liu, B. L.; Wang, X.; Gui, H.; Yuan, Y.; Zhai, S.; Ng, K. A.; Zhou, C. W.; Chen, Y. (9, 8) Single-Walled Carbon Nanotube Enrichment *via* Aqueous Two-Phase Separation and Their Thin-Film Transistor Applications. *Adv. Electron. Mater.* **2015**, *1*, 1500151.
(110) Hata, T.; Kawai, H.; Ohto, T.; Yamashita, K. Chirality Dependence of Quantum Thermal Transport in Carbon Nanotubes at Low Temperatures: A First-Principles Study. *J. Chem. Phys.* **2013**, *139*, 044711.
(111) Rajter, R. F.; French, R. H.; Ching, W. Y.; Podgornik, R.; Parsegian, V. A. Chirality-Dependent Properties of Carbon Nanotubes: Electronic Structure, Optical Dispersion Properties, Hamaker Coefficients and Van Der Waals−London Dispersion Interactions. *RSC Adv.* **2013**, *3*, 823−842.
(112) Joselevich, E. Electronic Structure and Chemical Reactivity of Carbon Nanotubes: A Chemist's View. *ChemPhysChem* **2004**, *5*, 619−624.
(113) Miyata, Y.; Kawai, T.; Miyamoto, Y.; Yanagi, K.; Maniwa, Y.; Kataura, H. Chirality-Dependent Combustion of Single-Walled Carbon Nanotubes. *J. Phys. Chem. C* **2007**, *111*, 9671−9677.
(114) Skandani, A. A.; Zeineldin, R.; Al-Haik, M. Effect of Chirality and Length on the Penetrability of Single-Walled Carbon Nanotubes into Lipid Bilayer Cell Membranes. *Langmuir* **2012**, *28*, 7872−7879.
(115) Odom, T. W.; Huang, J. L.; Kim, P.; Lieber, C. M. Atomic Structure and Electronic Properties of Single-Walled Carbon Nanotubes. *Nature* **1998**, *391*, 62−64.

DOI: 10.1021/acsnano.6b06900
ACS Nano XXXX, XXX, XXX−XXX

(116) Wilder, J. W. G.; Venema, L. C.; Rinzler, A. G.; Smalley, R. E.; Dekker, C. Electronic Structure of Atomically Resolved Carbon Nanotubes. *Nature* **1998**, *391*, 59−62.
(117) Hong, G.; Zhang, B.; Peng, B. H.; Zhang, J.; Choi, W. M.; Choi, J. Y.; Kim, J. M.; Liu, Z. F. Direct Growth of Semiconducting Single-Walled Carbon Nanotube Array. *J. Am. Chem. Soc.* **2009**, *131*, 14642−14643.
(118) Matsuda, Y.; Tahir-Kheli, J.; Goddard, W. A. Definitive Band Gaps for Single-Wall Carbon Nanotubes. *J. Phys. Chem. Lett.* **2010**, *1*, 2946−2950.
(119) Zhang, L.; Tu, X.; Welsher, K.; Wang, X. R.; Zheng, M.; Dai, H. Optical Characterizations and Electronic Devices of Nearly Pure (10,5) Single-Walled Carbon Nanotubes. *J. Am. Chem. Soc.* **2009**, *131*, 2454−2455.
(120) Telg, H.; Duque, J. G.; Staiger, M.; Tu, X.; Hennrich, F.; Kappes, M.; Zheng, M.; Maultzsch, J.; Thomsen, C.; Doorn, S. K. Chiral Index Dependence of the G^+ and G^- Raman Modes in Semiconducting Carbon Nanotubes. *ACS Nano* **2012**, *6*, 904−911.
(121) Haroz, E.; Duque, J. G.; Tu, X.; Zheng, M.; Walker, A. R. H.; Hauge, R.; Doorn, S. K.; Kono, J. Fundamental Optical Processes in Armchair Carbon Nanotubes. *Nanoscale* **2013**, *5*, 1411−1439.
(122) Mehlenbacher, R. D.; McDonough, T. J.; Grechko, M.; Wu, M. Y.; Arnold, M. S.; Zanni, M. T. Energy Transfer Pathways in Semiconducting Carbon Nanotubes Revealed Using Two-Dimensional White-Light Spectroscopy. *Nat. Commun.* **2015**, *6*, 6732.
(123) Jain, R. M.; Howden, R.; Tvrdy, K.; Shimizu, S.; Hilmer, A. J.; McNicholas, T. P.; Gleason, K. K.; Strano, M. S. Polymer-Free Near-Infrared Photovoltaics with Single Chirality (6,5) Semiconducting Carbon Nanotube Active Layers. *Adv. Mater.* **2012**, *24*, 4436−4439.
(124) Isborn, C. M.; Tang, C.; Martini, A.; Johnson, E. R.; Otero-de-la-Roza, A.; Tung, V. C. Carbon Nanotube Chirality Determines Efficiency of Electron Transfer to Fullerene in All-Carbon Photovoltaics. *J. Phys. Chem. Lett.* **2013**, *4*, 2914−2918.
(125) Gong, M.; Shastry, T. A.; Xie, Y.; Bernardi, M.; Jasion, D.; Luck, K. A.; Marks, T. J.; Grossman, J. C.; Ren, S.; Hersam, M. C. Polychiral Semiconducting Carbon Nanotube-Fullerene Solar Cells. *Nano Lett.* **2014**, *14*, 5308−5314.
(126) Ferguson, A. J.; Dowgiallo, A.-M.; Bindl, D. J.; Mistry, K. S.; Reid, O. G.; Kopidakis, N.; Arnold, M. S.; Blackburn, J. L. Trap-Limited Carrier Recombination in Single-Walled Carbon Nanotube Heterojunctions with Fullerene Acceptor Layers. *Phys. Rev. B: Condens. Matter Mater. Phys.* **2015**, *91*, 245311.
(127) Pfohl, M.; Glaser, K.; Graf, A.; Mertens, A.; Tune, D. D.; Puerckhauer, T.; Alam, A.; Wei, L.; Chen, Y.; Zaumseil, J.; Colsmann, A.; Krupke, R.; Flavel, B. S. Probing the Diameter Limit of Single Walled Carbon Nanotubes in SWCNT: Fullerene Solar Cells. *Adv. Energy Mater.* **2016**, *6*, 1600890.
(128) Arnold, M. S.; Blackburn, J. L.; Crochet, J. J.; Doorn, S. K.; Duque, J. G.; Mohite, A.; Telg, H. Recent Developments in the Photophysics of Single-Walled Carbon Nanotubes for Their Use as Active and Passive Material Elements in Thin Film Photovoltaics. *Phys. Chem. Chem. Phys.* **2013**, *15*, 14896−14918.
(129) Tanaka, Y.; Hirana, Y.; Niidome, Y.; Kato, K.; Saito, S.; Nakashima, N. Experimentally Determined Redox Potentials of Individual (n,m) Single-Walled Carbon Nanotubes. *Angew. Chem., Int. Ed.* **2009**, *48*, 7655−7659.
(130) Jariwala, D.; Sangwan, V. K.; Wu, C. C.; Prabhumirashi, P. L.; Geier, M. L.; Marks, T. J.; Lauhon, L. J.; Hersam, M. C. Gate-Tunable Carbon Nanotube-MoS_2 Heterojunction p-n Diode. *Proc. Natl. Acad. Sci. U. S. A.* **2013**, *110*, 18076−18080.
(131) Cui, X. D.; Freitag, M.; Martel, R.; Brus, L.; Avouris, P. Controlling Energy-Level Alignments at Carbon Nanotube/Au Contacts. *Nano Lett.* **2003**, *3*, 783−787.
(132) Antaris, A. L.; Robinson, J. T.; Yaghi, O. K.; Hong, G. S.; Diao, S.; Luong, R.; Dai, H. J. Ultra-Low Doses of Chirality Sorted (6,5) Carbon Nanotubes for Simultaneous Tumor Imaging and Photothermal Therapy. *ACS Nano* **2013**, *7*, 3644−3652.
(133) Diao, S.; Hong, G. S.; Robinson, J. T.; Jiao, L. Y.; Antaris, A. L.; Wu, J. Z.; Choi, C. L.; Dai, H. J. Chirality Enriched (12,1) and (11,3) Single-Walled Carbon Nanotubes for Biological Imaging. *J. Am. Chem. Soc.* **2012**, *134*, 16971−16974.
(134) Hong, G. S.; Diao, S. O.; Antaris, A. L.; Dai, H. J. Carbon Nanomaterials for Biological Imaging and Nanomedicinal Therapy. *Chem. Rev.* **2015**, *115*, 10816−10906.
(135) Antaris, A. L.; Yaghi, O. K.; Hong, G. S.; Diao, S.; Zhang, B.; Yang, J.; Chew, L.; Dai, H. J. Single Chirality (6,4) Single-Walled Carbon Nanotubes for Fluorescence Imaging with Silicon Detectors. *Small* **2015**, *11*, 6325−6330.
(136) Acosta, V.; Hemmer, P. Nitrogen-Vacancy Centers: Physics and Applications. *MRS Bull.* **2013**, *38*, 127−130.
(137) He, Y. M.; Clark, G.; Schaibley, J. R.; He, Y.; Chen, M. C.; Wei, Y. J.; Ding, X.; Zhang, Q.; Yao, W.; Xu, X.; Lu, C. Y.; Pan, J. W. Single Quantum Emitters in Monolayer Semiconductors. *Nat. Nanotechnol.* **2015**, *10*, 497−502.
(138) Ma, X.; Hartmann, N. F.; Baldwin, J. K.; Doorn, S. K.; Htoon, H. Room-Temperature Single-Photon Generation from Solitary Dopants of Carbon Nanotubes. *Nat. Nanotechnol.* **2015**, *10*, 671−675.
(139) Tang, Z. K.; Zhai, J. P.; Tong, Y. Y.; Hu, X. J.; Saito, R.; Feng, Y. J.; Sheng, P. Resonant Raman Scattering of the Smallest Single-walled Carbon Nanotubes. *Phys. Rev. Lett.* **2008**, *101*, 047402.
(140) Wang, Q.; Yang, S. W.; Yang, Y. H.; Chan-Park, M. B.; Chen, Y. Charge Transfer between Metal Clusters and Growing Carbon Structures in Chirality-Controlled Single-Walled Carbon Nanotube Growth. *J. Phys. Chem. Lett.* **2011**, *2*, 1009−1014.
(141) Wang, J. T.; Liu, P.; Xia, B. Y.; Wei, H. M.; Wei, Y.; Wu, Y.; Liu, K.; Zhang, L. N.; Wang, J. P.; Li, Q. Q.; Fan, S. S.; Jiang, K. L. Observation of Charge Generation and Transfer During CVD Growth of Carbon Nanotubes. *Nano Lett.* **2016**, *16*, 4102−4109.
(142) Chen, Y. B.; Shen, Z. Y.; Xu, Z. W.; Hu, Y.; Xu, H. T.; Wang, S.; Guo, X. L.; Zhang, Y. F.; Peng, L. M.; Ding, F.; Liu, Z. F.; Zhang, J. Helicity-Dependent Single-Walled Carbon Nanotube Alignment on Graphite for Helical Angle and Handedness Recognition. *Nat. Commun.* **2013**, *4*, 2205.
(143) Ao, G.; Streit, J. K.; Fagan, J. A.; Zheng, M. Differentiating Left- and Right-Handed Carbon Nanotubes by DNA. *J. Am. Chem. Soc.* **2016**, *138*, 16677.
(144) Maruyama, T.; Kondo, H.; Ghosh, R.; Kozawa, A.; Naritsuka, S.; Iizumi, Y.; Okazaki, T.; Iijima, S. Single-Walled Carbon Nanotube Synthesis Using Pt Catalysts Under Low Ethanol Pressure *via* Cold-Wall Chemical Vapor Deposition in High Vacuum. *Carbon* **2016**, *96*, 6−13.

DOI: 10.1021/acsnano.6b06900
ACS Nano XXXX, XXX, XXX−XXX